Synthesis and Investigation of Chiral Poly(2,4-disubstituted-2-oxazoline)-Based Triblock Copolymers, Their Self-Assembly, and Formulation with Chiral and Achiral Drugs

Yang, Mengshi

2022-07-26

Yang , M , Haider , M S , Forster , S , Hu , C & Luxenhofer , R 2022 , ' Synthesis and Investigation of Chiral Poly(2,4-disubstituted-2-oxazoline)-Based Triblock Copolymers, Their Self-Assembly, and Formulation with Chiral and Achiral Drugs ' , Macromolecules , vol. 55 , no. 14 , pp. 6176-6190 . https://doi.org/10.1021/acs.macromol.2c00229

http://hdl.handle.net/10138/346745
https://doi.org/10.1021/acs.macromol.2c00229

Macromolecules

pubs.acs.org/Macromolecules Article

Synthesis and Investigation of Chiral Poly(2,4-disubstituted-2-oxazoline)-Based Triblock Copolymers, Their Self-Assembly, and Formulation with Chiral and Achiral Drugs

Mengshi Yang, Malik Salman Haider, Stefan Forster, Chen Hu, and Robert Luxenhofer*

Cite This: *Macromolecules* 2022, 55, 6176–6190 Read Online

ACCESS | Metrics & More | Article Recommendations | Supporting Information

ABSTRACT: Considering the largely chiral nature of biological systems, there is interest in chiral drug delivery systems. Here, we investigate for the first time polymer micelles based on poly(2-oxazoline) (POx) ABA-type triblock copolymers with chiral and racemic hydrophobic blocks for the formulation of chiral and achiral drugs. Specifically, poly(2-ethyl-4-ethyl-2-oxazoline) (pEtEtOx) and poly(2-propyl-4-methyl-2-oxazoline) (pPrMeOx) were used as hydrophobic block B and poly(2-methyl-2-oxazoline) (pMeOx) as hydrophilic block A. Using these triblock copolymers, nanoformulations of curcumin (CUR), paclitaxel (PTX), and chiral (*R* and *S*) and racemic ibuprofen were prepared. For CUR and PTX, the maximum drug loading was significantly dependent on the structure of the hydrophobic repeat units, but not the chirality. In contrast, the maximum drug loading with chiral/racemic ibuprofen was affected neither by the polymer structure nor by chirality, but minor effects were observed with respect to the size and size distribution of the drug-loaded micelles.

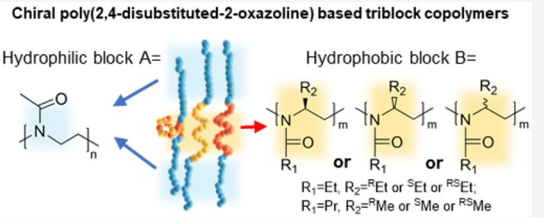

INTRODUCTION

Chirality is an essential property for many biologically relevant molecules, including bio(macro)molecules such as sugars, amino acids, and their polymers (proteins, polysaccharides, DNA/RNA). Despite the seemingly minute structural difference, enantiomers of drugs can exhibit significant differences in their biological activity such as pharmacology abdtoxicology etc.[1] For instance, for the analgesic drug ibuprofen, its *S*-enantiomer has a higher efficacy than its stereoisomer.[1] In the worst case, a stereoisomer can produce undesired or toxic effects. A notorious example is thalidomide, which was first marketed in 1957 as a racemic mixture, but due to severe teratogenic effects (phocomelia, amelia) caused by its *S*-enantiomer, it was withdrawn from the market in the early 1960s.[1] Therefore, the isolation of therapeutically active enantiomers is of utmost importance. Chiral resolution can be achieved, *inter alia*, by chiral chromatography, in which a chiral compound is immobilized on the surface of the stationary phase.[2] Accordingly, it may appear logical to utilize chiral drug delivery systems to also preferentially interact/solubilize a drug enantiomer of interest. Therefore, synthetic stereoactive polymers, in which repeating units feature chiral centers, have attracted some attention. Recent studies on poly(lactide) (PLA)-,[3] poly(glutamic acid)-,[4] and poly(leucine)-based block copolymers[5] have reported the effect of polymer stereoregularity on the physicochemical and functional properties of their self-assembled nanostructures.[6] Feng et al. investigated micelles based on methoxy-poly(ethylene glycol)-*b*-poly(L-lactide) micelles (mPEG-*b*-PLLA, L-micelles) and mPEG-*b*-poly(D-lactide) micelles (mPEG-*b*-PDLA, D-micelles) to solubilize the glycosylated antibiotic nocathiacin I (containing multiple chiral centers) and other chiral compounds (containing D- or L-sugars).[7] They observed that the nocathiacin I-loaded D-micelles exhibited better loading efficiency and smaller particle size than those of L-micelles. Also, for micelles loaded with other chiral compounds, D- and L-micelles showed a marked difference in particle size, even though the loading efficiency between D- and L-micelles was not significantly different. Hu et al. loaded insulin in stereo multiblock copoly(lactide)s (smb-PLAs) with different stereoregularity.[8] They found that smb-PLAs with a high stereoregularity show much higher insulin loading efficiency than the atactic PLA. In addition to stereoregularity, the rigidity of the chiral chain also impacts the polymer properties. Nguyen et al. developed sets of chiral bottlebrush polymers (CBPs) based on unimolecular norbornene-terminated macromonomers (MMs) with different stereochemistry and rigidity.[9] The stereoregularity influenced the CBPs with flexible chiral side chains remarkably in cytotoxicity, cell uptake, blood pharmacokinetics, and liver clearance. However, the CBPs with a comparably rigid chiral side chain did not

Received: January 29, 2022
Revised: April 6, 2022
Published: July 7, 2022

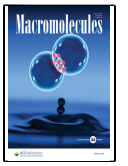

Scheme 1. (a) Chemical Structures of the A−B−A Triblock Copolymers Used in This Study, Where Hydrophilic Blocks A Are Poly(2-methyl-2-oxazoline) (pMeOx) and the Hydrophobic Block B is Poly(2-ethyl-4-ethyl-2-oxazoline) (p^{R}EtEtOx, p^{S}EtEtOx, p^{RS}EtEtOx) or Poly(2-propyl-4-methyl-2-oxazoline) (p^{R}PrMeOx, p^{S}PrMeOx, p^{RS}PrMeOx). (b) Chemical Structure of the Model Drugs Used in This Study, Paclitaxel, Curcumin, and Ibuprofen. (c) Schematic Representation of the Formulation Procedure (Thin-Film Method)

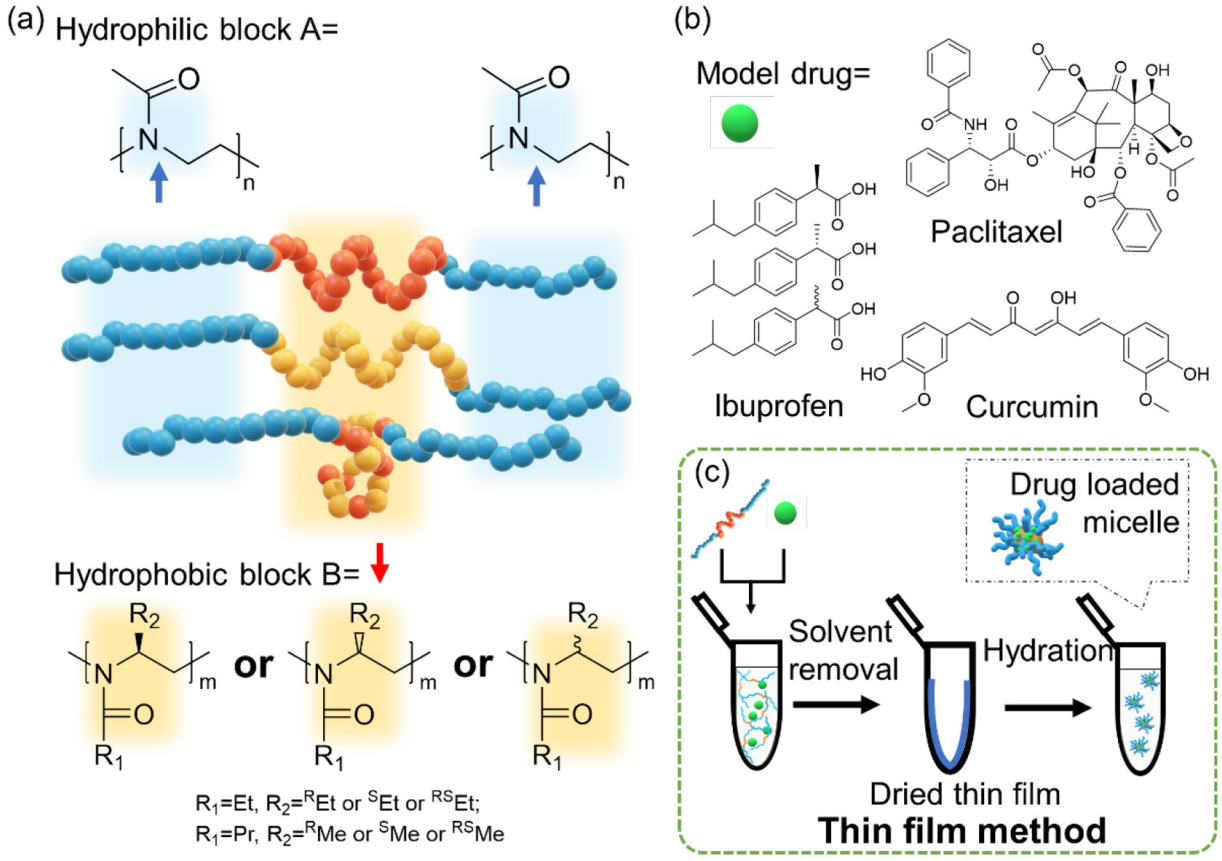

show an obvious difference between isomers. Apparently, the bigger conformational flexibility amplifies the diastereomeric interactions. In general, how polymer stereoregular blocks change the properties such as micellar size, micellar thermodynamic stability, drug loading, and cell interaction is generally not broadly investigated and understood.

Poly(2-oxazoline)s (POx) are a family of polymers of the larger group of polymers classified as pseudo-polypeptides. In the past two decades, POx have gained increasing interest for a wide range of applications, especially in the biomedical field, e.g., drug, protein, and gene delivery, tissue engineering, regenerative medicine, 3D bioprinting, and biofabrication.[10,11] The 2-oxazoline monomers with different substituents in the 2-position can be tailor-made by a relatively easy and straightforward synthesis,[12−14] and numerous monomers have been used in cationic ring-opening polymerization to obtain the corresponding poly(2-alkyl/aryl-2-oxazoline)s with narrow molar mass distributions and a wide range of physicochemical properties.[11,15−17] Among them, the hydrophilic POx poly(2-methyl-2-oxazoline)s (pMeOx) and poly(2-ethyl-2-oxazoline)s (pEtOx) have been studied intensively, as they exhibit stealth/protein-repellent effects.[18−21] They are regularly discussed as one of the potential alternatives to PEG.[11,20,22−25] Accordingly, pMeOx and pEtOx have been used widely as hydrophilic polymer components, e.g., in polymer nanoparticles[26] and micelles (in combination with other hydrophobic POx, e.g., with 2-butyl, 2-nonyl, or 2-isopropyl-2-oxazoline[27]), polymer−peptide conjugates,[28,29] polymer−protein conjugates,[30] lipopolymers for liposome stabilization,[19] polymer−drug conjugates,[31] and antimicrobial polymers.[32] While the toolbox of 2-substituted 2-oxazolines and their corresponding polymers has been expanding rapidly, however, work on monomers and polymers with additional substituents in the 4- and 5-position is quite limited.[33] The proof-of-principle that such 2,4-disubstituted POx are accessible was provided by Saegusa et al., who synthesized optically active poly(ethylenimine) derivatives by ring-opening polymerization of 4-substituted-2-oxazoline and 4,5-disubstituted-2-oxazoline for the first time.[34,35] Much later Schubert, Hoogenboom, and co-workers reported the synthesis and properties of chiral poly(2-R-4-ethyl-2-oxazoline)s (R = ethyl, butyl, octyl, nonyl, undecyl)[36−39] and further discussed the self-assembly of chiral amphiphilic block copolymers composed of a hydrophilic block of pEtOx and a hydrophobic block of poly((R)-2-butyl-4-ethyl-2-oxazoline) (p^{R}BuEtOx) or racemic p^{RS}BuEtOx.[40] They found that varying the hydrophobic/hydrophilic ratio in the copolymers could control the type of self-assembled structures from spherical and cylindrical micelles to sheets and vesicles. Unfortunately, in this contribution, no direct comparison of chiral and racemic polymers of the same composition was provided.[40] Jordan et al. investigated the influence of chirality on the lower critical

https://doi.org/10.1021/acs.macromol.2c00229
Macromolecules 2022, 55, 6176−6190

solution temperature (LCST) behavior of water-soluble poly(2-alkyl-4-methyl-2-oxazoline)s (alkyl: methyl, ethyl).[41] Introduction of chirality via the alkyl substituents in the main chain of poly(2,4-disubstituted-2-oxazoline)s allows for the formation of secondary structure in aqueous and nonaqueous environments as well as in bulk.[38,41] In a patent, Schmidt and Bott proposed a possible application of poly(4(S)-4-ethyl-2-phenyl-2-oxazoline) in the separation of enantiomeric mixtures of D,L-2-chloro-4-methylphenoxypropionic acid methyl ester.[42]

As many drugs, including hydrophobic ones, are chiral, it is interesting to study the effect of chirality on POx-based drug formulations. While in recent years significant structure−property relationships regarding hydrophobic drug formulations using a large variety of amphiphilic POx have been studied,[43−46] a drug formulation based on main chain chiral POx has not been studied before. Aiming to improve our understanding of stereoregular polymers as drug carriers in general and to enlarge the toolbox of POx-based drug formulations in particular, we have synthesized two series of chiral POx-based ABA amphiphilic triblock copolymers. We explored their potential application for drug formulation and their selectivity and affinity for particular drug enantiomers. Specifically, ABA triblock copolymers were synthesized via living cationic ring-opening polymerization (LCROP), comprising pMeOx as hydrophilic blocks A on the one hand and chiral poly((R)-2-ethyl-4-ethyl-2-oxazoline) (p^{R}EtEtOx), poly((S)-2-ethyl-4-ethyl-2-oxazoline) (p^{S}EtEtOx) and racemic poly((RS)-2-ethyl-4-ethyl-2-oxazoline) (p^{RS}EtEtOx) as well as poly((R)-2-propyl-4-methyl-2-oxazoline) (p^{R}PrMeOx), p^{S}PrMeOx, and p^{RS}PrMeOx as hydrophobic block B on the other hand. Their aqueous solubility, optical activity, thermal properties, and drug loading with respect to chirality were investigated. The corresponding hydrophobic homopolymers were also synthesized and investigated to help understand the properties of triblock copolymers. Curcumin (CUR) and paclitaxel (PTX) were used as models of common hydrophobic drugs, whereas *R*-ibuprofen (R-IBU), *S*-IBU, and *RS*-IBU were used as model compounds for chiral drugs and a racemic drug mixture.

EXPERIMENTAL SECTION

Materials. All substances for the preparation of the polymers were purchased from Sigma-Aldrich (Steinheim, Germany) or Acros (Geel, Belgium) and were used as received unless otherwise stated. D-Alaninol (purity 98%), (*S*)-(+)-2-amino-1-propanol (purity 98%), (*R*)-(−)-2-amino-1-butanol (purity 98%), and (*S*)-(+)-2-amino-1-butanol (purity 98%) were purchased from abcr (Karlsruhe, Germany). DL-2-Amino-1-propanol (purity 98%) and DL-2-amino-1-butanol (purity 98%) were purchased from TCI (Eschborn, Germany). Curcumin powder from *Curcuma longa* (turmeric) was purchased from Sigma-Aldrich (curcumin = 79%; demethoxycurcumin = 17%, bisdemethoxycurcumin = 4%; determined by HPLC analysis). Paclitaxel was purchased from LC Laboratories (Woburn, MA, USA). (*R*)-(−)-Ibuprofen (98.5%) was purchased from MedChemExpress (distributor Hycultec, Beutelsbach, Germany). (*S*)-(+)-Ibuprofen (99%) and racemic ibuprofen (pharmaceutical secondary standard; certified reference material) was purchased from Sigma-Aldrich. Deuterated solvents for NMR analysis were obtained from Deutero GmbH (Kastellaun, Germany).

The monomers (*R*)-2-ethyl-4-ethyl-2-oxazoline (^{R}EtEtOx), (*S*)-2-ethyl-4-ethyl-2-oxazoline (^{S}EtEtOx), (*RS*)-2-ethyl-4-ethyl-2-oxazoline (^{RS}EtEtOx), (*R*)-2-propyl-4-methyl-2-oxazoline (^{R}PrMeOx), (*S*)-2-propyl-4-methyl-2-oxazoline (^{S}PrMeOx), and (*RS*)-2-propyl-4-methyl-2-oxazoline (^{RS}PrMeOx) were prepared following the procedure by Witte and Seeliger et al.[12,13] For monomer synthesis and characterization, see Figures S1−S4 in the Supporting Information (SI). The substances used for polymerization, specifically methyl trifluoromethylsulfonate (MeOTf), 2-methyl-2-oxazoline (MeOx), ^{R}EtEtOx, ^{S}EtEtOx, ^{RS}EtEtOx, ^{R}PrMeOx, ^{S}PrMeOx, ^{RS}PrMeOx, and sulfolane, were refluxed over CaH_2, distilled, and stored under argon.

Polymer Synthesis. The polymerization and workup procedures were carried out similar to those of Lübtow et al. described previously.[44] The initiator MeOTf was added to a dried and argon-flushed flask and mixed with the respective volume of sulfolane, followed by monomer addition. Subsequently, the reaction mixture was heated to 100 or 130 °C (according to the type of monomers, see SI). Reaction progress was controlled by ^{1}H NMR spectroscopy. After complete consumption of monomer, additional monomer was added in case of block copolymer synthesis, or termination was carried out by addition of 1-Boc-piperazine (PipBoc) at 50 °C. Subsequently, K_2CO_3 was added, and the mixture was stirred at 50 °C. The crude product was purified by dialysis. For polymer synthesis details and characterization, see Figures S5−S7 and Figures S11 and S12 in SI.

Nuclear Magnetic Resonance Spectroscopy. NMR spectra were measured with a Fourier 300 (^{1}H, 300 MHz; ^{13}C, 75 MHz) Bruker Biospin (Rheinstetten, Germany) at 298 K. All chemical shifts are given in ppm. The spectra were calibrated to the signals of residual protonated solvent signals (e.g., $CDCl_3$ in ^{1}H NMR: 7.26 ppm; in ^{13}C NMR: 77.06 ppm).

Size Exclusion Chromatography (SEC). SEC of polymers was performed on an Agilent 1260 Infinity System, Polymer Standard Service (Mainz, Germany), with hexafluoroisopropanol (HFIP) containing 3 g/L potassium trifluoroacetate; precolumn: 50 mm × 8 mm PSS PFG linear M (particle size 7 μm); main column: 8 × 300 mm AppliChrom ABOA HFIP-P350 (pore size 0.1−1000 kDa). The columns were kept at 40 °C, and the flow rate was 0.3 mL/min. Prior to each measurement, samples were dissolved in HFIP/potassium trifluoroacetate and filtered through 0.2 μm PTFE filters, Roth (Karlsruhe, Germany). Conventional calibration was performed with PEG standards (0.1−1000 kg/mol), and data were processed with Win-GPC software.

SEC of pPrMeOx homopolymers was also performed on an alternative SEC system, a Malvern GPCMax system (Malvern, UK), with a VE 3580 RI detector, PSS Polymer Standard Service (Mainz, Germany); two Malvern LC4000L column: 300 × 8 mm (exclusion limit: 400 kDa). Chloroform was used as the eluent with a 100 μL sample volume injection. The columns were kept at 35 °C, and the flow rate was 1 mL/min. Prior to each measurement, samples were dissolved in chloroform and filtered through 0.2 μm PTFE filters, Roth (Karlsruhe, Germany). Conventional calibration was performed with polystyrene standards (1.2−40 kDa), and data were processed with OmniSEC software.

Thermogravimetric Analysis (TGA). A TG 209 F1 IRIS, Netzsch (Selb, Germany), was used for thermal analysis. The samples (5−10 mg) were added into aluminum oxide crucibles (Netzsch) and heated under synthetic air from 30 to 900 °C (10 °C/min) while detecting the mass loss.

Differential Scanning Calorimetry (DSC). DSC was performed on a DSC 204 F1 Phoenix, Netzsch, under a N_2 atmosphere (20.0 mL/min). The samples were placed in aluminum pans with pierced crimped-on lids, heated from 30 to 190 °C, and subsequently cooled to −50 °C (10 °C/min). The heating/cooling cycle was repeated two additional times from −50 to 190 °C (10 °C/min).

X-ray Diffraction (XRD). XRD measurements were performed on a D8 Advance diffractometer with DaVinci design (Bruker AXS, Karlsruhe, Germany). The following measurement parameters were applied: a 2θ range of 5−60°, a step size of 0.02° 2θ, an integration time of 2 s, copper Kα radiation, generator settings of 20 kV and 5 mA and a 0.344° divergence slit. The data were exported by the software DIFFRAC.EVA (Bruker AXS, Karlsruhe, Germany).

Fluorescence Spectroscopy−Critical Micelle Concentration (CMC). The CMC of triblock copolymers was determined using the fluorescence probe pyrene. Pyrene solutions (24 μM, 5.0 mg/L in acetone) were added to glass vials followed by acetone removal by a gentle stream of argon. Afterward, various amounts of aqueous

https://doi.org/10.1021/acs.macromol.2c00229
Macromolecules 2022, 55, 6176−6190

polymer stock solutions were added, and the solutions were diluted with water (Millipore) to yield a final pyrene concentration of 5×10^{-7} M. The samples were shaken gently for 30 min and stored overnight at ambient temperature (~20 °C) under the exclusion of light. Fluorescence measurements were performed in an FP-8300, Jasco, from 360 to 400 nm (λ_{ex} = 333 nm) at 25 °C with 10 × 10 mm fluorescence cuvettes.

The fluorescence spectrum of pyrene shows five characteristic vibronic bands around 360−400 nm.[47] The ratio of the fluorescence intensities of the first and third vibronic bands of pyrene (I_1:I_3 ratio) increases characteristically with increasing polarity of the probe environment.[42] The CMC was determined as the concentration at which the fitted I_1:I_3 ratio decreased to 90% of its initial value.[48]

Circular Dichroism (CD) Characterization. CD spectra were measured in methanol or water solutions (0.1 g/L polymer concentration) with a JASCO J-810 circular dichroism spectrometer (JASCO International Co., Ltd., Tokyo, Japan). The following scanning conditions were used: 200 nm/min scanning rate; 1 nm bandwidth; 0.5 nm data pitch; 1 s response time; and 3 accumulations. Samples were measured in a 1 mm path length quartz cuvette (110-QS, Hellma Analytics).

Drug Formulation. Drug-loaded polymer micelles were prepared using the thin-film hydration method.[44] Ethanolic polymer (20 g/L), curcumin (5 g/L), paclitaxel (5 g/L), and *R*-IBU (5 g/L), *S*-IBU (5 g/L), or *RS*-IBU (5 g/L) stock solutions were mixed in the desired ratio. After complete removal of the solvent at 50 °C under a mild stream of argon, the films were further dried under vacuum (≤0.2 mbar) for at least 30 min. Subsequently, preheated (37 °C) H_2O (Millipore) was added to obtain the final polymer (10 g/L) and desired drug concentrations. To ensure complete solubilization, the solutions were shaken at 55 °C for 15 min, at 1250 rpm with a Thermomixer Comfort (Eppendorf AG, Hamburg, Germany). Nonsolubilized drug was removed by centrifugation for 5 min at 9000 rpm (relative centrifugal force (rcf) 7788g) by a MIKRO 185 (Hettich, Tuttlingen, Germany). The solubilization experiments were performed with three individually prepared samples, and results are presented as means ± standard deviation (SD).

The loading capacity (LC) and loading efficiency (LE) were calculated using the following equations:

$$\mathrm{LC} = \frac{m_{\mathrm{drug}}}{m_{\mathrm{drug}} + m_{\mathrm{polymer}}} \times 100\%$$

$$\mathrm{LE} = \frac{m_{\mathrm{drug}}}{m_{\mathrm{drug,added}}} \times 100\%$$

where m_{drug} and $m_{polymer}$ are the weight amounts of the solubilized drug and polymer excipient in solution and $m_{drug,added}$ is the weight amount of the drug initially added to the dispersion. No loss of polymer during micelle preparation was assumed.

UV−Vis Spectroscopy. CUR quantification was performed by UV−vis absorption on a BioTek Eon microplate spectrophotometer, Thermo Fisher Scientific (Waltham, MA, USA), using a calibration curve obtained with known amounts of CUR, dissolved in ethanol. Samples were prepared in Rotilabo F-Type 96-well plates, Carl Roth GmbH & Co. KG (Karlsruhe, Germany), at a constant volume of 200 μL. Spectra were recorded from 300 to 700 nm at 25 °C. Curcumin absorption was detected at 430 nm. Prior to UV−vis absorption measurements, the aqueous formulations were appropriately diluted with ethanol to give a final absorbance between 0.3 and 2.5 (diluted at least 1/20 (v/v)).

High-Performance Liquid Chromatography (HPLC) Analysis. HPLC analysis was carried out using a Prominence LC-20A modular HPLC system (Shimadzu, Duisburg, Germany) equipped with a CBM-20A system controller, an LC-20 AT solvent delivery unit (double plunger), a DGU-20A online degassing unit, a SIL-20AC autosampler, an SPD-M20A photodiode array detector, a CTO-20AC column oven, and a RID-20A refractive index detector. As stationary phase, a Zorbax Eclipse Plus, Agilent (Santa Clara, CA, USA) C18 column (4.6 × 100 mm; 3.5 μm50 mm × 4 mm) was used. The volume of samples injected was 20 μL, and elution was performed using a mobile phase of H_2O and acetonitrile (ACN) containing 0.05% trifluoroacetic acid (TFA) at 40 °C and a flow rate of 1 mL/min.

Quantification of PTX and IBU was performed at 220 nm.[49−51] For PTX, within the first 10 min, the proportion of ACN was increased from 40% to 60%. Solvent proportion was kept constant for 5 min prior to decreasing it to the initial proportion of 40% ACN within 0.5 min. For IBU, the proportion of ACN was increased from 40% to 60% ACN within the first 10 min, afterward it was increased to 80% ACN in 0.1 min and kept constant for 1.9 min, and finally it was decreased to the initial proportion of 40% ACN in 0.1 min. The retention times were 8.2 min for PTX and 9.5 min for IBU.

Dynamic Light Scattering (DLS). Triblock copolymer aqueous solutions and CUR- or IBU-loaded formulations were prepared with PBS (pH 7.4) and measured on a Zetasizer Nano ZSP from Malvern (Malvern Instruments, Worcestershire, UK) in disposable cuvettes (UV cuvettes semi micro, Brand GmbH, Wertheim, Germany) at ambient temperature (~25 °C). Data were analyzed by using Zetasizer software 7.11. All samples were measured after filtration using a 0.45 μm PVDF syringe filter (Rotilabo, Karlsruhe). The filtered samples were further diluted with PBS and measured again to exclude variation due to a dilution effect. The data presentedare the average of three measurements.

Long-Term Stability Studies. For long-term stability studies, formulated IBU was stored at ambient conditions (~25 °C). The samples were collected at day 0, 1, 8, 20, 30, and 60. Before the determination of the drug loading by HPLC, all samples were centrifuged for 5 min at 9000 rpm (rcf 7788 g)with a MIKRO 185 (Hettich, Tuttlingen, Germany). Long-term stabilization experiments were performed with three individually prepared samples, and results are presented as means ± SD; quantification was carried out as described previously.

Statistical Analysis. Statistical significance was calculated by Student's *t* test. Differences with a value of $p < 0.05$ were considered statistically significant.

RESULTS AND DISCUSSION

Synthesis and Characterization of Homopolymers. The EtEtOx and PrMeOx series monomers were prepared following the procedure by Witte and Seeliger et al.[12,13] Nitrile and chiral or achiral alkanolamine were heated for 2−6 d under the catalysis of zinc acetate dihydrate to produce the corresponding monomers. A detailed description of monomer synthesis and characterization can be found in SI, Figures S1−S4.

Since synthesis of poly(2-propyl-4-methyl-2-oxazoline) (pPrMeOx) and its characteristics were not reported before, the respective homopolymers were synthesized and characterized first. Knowledge of the homopolymerization and homopolymer properties is also important to support the synthesis of corresponding polymer amphiphiles and their characterization. Also, this allows a direct comparison with its isomer pEtEtOx. Accordingly, the homopolymers p^{R}EtEtOx, p^{S}EtEtOx, p^{RS}EtEtOx, p^{R}PrMeOx, p^{S}PrMeOx, and p^{RS}PrMeOx were prepared by LCROP. Using a $[M]_0/[I]_0$ = 20, the complete polymerization of monomers ^{R}EtEtOx, ^{S}EtEtOx, and ^{RS}EtEtOx was achieved after about 45 h at 130 °C. In comparison, the monomer consumption for ^{R}PrMeOx, ^{S}PrMeOx, and ^{RS}PrMeOx was complete after only approximately 24 h at 130 °C, which can be attributed to decreased steric hindrance due to the smaller Me substituent at the 4-position, affecting the nucleophilic attack of monomer at the 5-position. We tested the solubility of homopolymers in different solvents. All these homopolymers are well soluble in HFIP (≥5 g/L) and excellently soluble in chloroform, methanol, and

https://doi.org/10.1021/acs.macromol.2c00229
Macromolecules 2022, 55, 6176−6190

Table 1. Physicochemical Characterization of Synthesized Homopolymers Including the Yield, Number Average Molecular Weight M_n, Dispersity $Đ$, and the Extrapolated Onset Temperature of Major Mass Loss T_d

polymer	yield [%]	M_n[a] [kg mol^{-1}]	M_n[b] [kg mol^{-1}]	M_n[c] [kg mol^{-1}]	$Đ$[c]	T_d[d] [°C]	solubility[e]
p^{R}EtEtOx	69.3	2.7	2.9	1.3*	1.09*	362	7.8
p^{S}EtEtOx	90.5	2.7	3.1	1.0*	1.16*	345	7.8
p^{RS}EtEtOx	57.7	2.8	2.9	1.2*	1.13*	361	9.4
p^{R}PrMeOx	76.0	2.8	3.0	1.3*	1.10 *	357	9.3
				3.5‡	1.13‡		
p^{S}PrMeOx	86.6	2.8	3.0	1.3*	1.09*	344	8.9
				3.2‡	1.10‡		
p^{RS}PrMeOx	78.3	2.8	3.1	1.0*	1.11*	351	9.9
				3.0‡	1.09‡		

[a]Theoretical molar mass from $[M]_0/[I]_0$. [b]As obtained by ^{1}H NMR ($CDCl_3$; 300 MHz) evaluated as mean of all relevant integral ratios. [c]As obtained by SEC (*eluent: HFIP, calibrated with PEG standards; ‡eluent: chloroform, calibrated with polystyrene). [d]Extrapolated onset temperature of major mass loss (TGA). [e]Solubility in water at 4 °C in g/L.

ethanol (all ≥200 g/L), but poorly soluble in water (<0.5 g/L in water) at room temperature. The poor water solubility is roughly in line with the well-known side chain size dependence of POx solubility.[52] Interestingly, when the saturated aqueous solutions of the homopolymers equilibrated at 4 °C were brought to room temperature, the previously clear solutions turned turbid. The concentration of the saturated aqueous solutions at 4 °C was determined to be 8−10 g/L (Table 1), and therefore pEtEtOx and pPrMeOx show an LCST behavior. This is well known of course for POx and poly(2-alkyl-2-oxazines) (POzi) with C3 side chains, such as poly(2-propyl-2-oxazoline) (pPrOx), poly(2-isopropyl-2-oxazoline) (p*i*PrOx), poly(2-propyl-2-oxazine) (pPrOzi), and poly(2-isopropyl-2-oxazine) (p*i*PrOzi),[53−55] but to the best of our knowledge has not been described for either POx or POzi with side chains comprising four carbon atoms.

The homopolymers were further characterized by ^{1}H NMR and SEC, the results of which are detailed in the SI (Figures S5−S9) and Table 1. The polymerization was terminated with PipBoc, wherein the Boc moiety yields a sharp and intense singlet in the ^{1}H NMR spectrum (Figures S6 and S7), facilitating end-group analysis. Based on this, p^{R}EtEtOx, p^{S}EtEtOx, and p^{RS}EtEtOx have a degree of polymerization (DP) of 21, 23, and 21, respectively, while p^{R}PrMeOx, p^{S}PrMeOx, and p^{RS}PrMeOx have a DP of 22, 22, and 23, respectively. Both the pEtEtOx and pPrMeOx series are reasonably close to the targeted DP of 20 (from monomer to initiator ratio $[M]_0$:$[I]_0$), but it must be noted that all polymer signals are very broad and overlapping, making an accurate end-group analysis difficult. The dispersity as determined by SEC (Table 1, Figure S8a and b) was very low with values of $Đ$ = 1.09−1.16. The molar mass obtained from SEC is considerably smaller than from end-group analysis by ^{1}H NMR, which can be attributed to a different solution behavior in the eluent compared to the utilized PEG standards used for calibration in SEC. Besides, the pPrMeOx series was also characterized using another SEC system (chloroform as eluent), to elucidate the effects of eluent and calibration standard (Figure S8c). This yielded considerable higher apparent molar masses.

To investigate the thermal stability of homopolymers, TGA was performed in the temperature range of 30 to 900 °C (Figure S9). Around 220 °C, 3−4% mass loss was observed in all homopolymers, which is consistent with the Boc weight percent of homopolymers.[56] The onset temperature of major mass loss T_d of all homopolymers is around 350 °C, which is consistent with the widely reported thermal stability of POx-based polymers.[45,57]

DSC measurements were performed from −50 to 190 °C in order to determine the thermal transitions of the homopolymers. In the given temperature range, no melting temperature (T_m) of homopolymers was observed (Figure 1), which may be

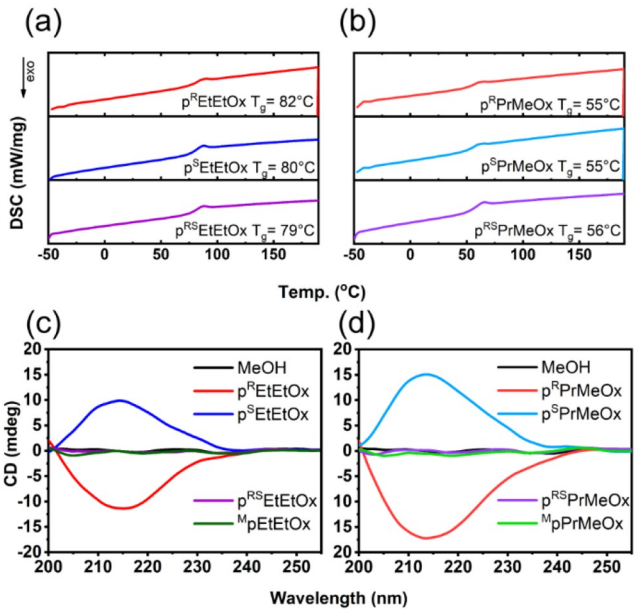

Figure 1. DSC heat flow of the third heating cycle of homopolymers (a) pEtEtOx and (b) pPrMeOx series. The samples were heated three times and cooled two times from −50 to 190 °C (10 °C/min). CD spectra of (c) pEtEtOx and (d) pPrMeOx series in methanol at 25 °C (polymer concentration was 0.1 g/L).

connected to the rather short side chain length. Normally, the POx with C4 side chains begin to show T_m.[58] The melt transitions of structural isomer p*i*PrOzi are not observed in DSC.[55] The glass transition temperatures (T_g) of pEtEtOx series homopolymers, p^{R}EtEtOx, p^{S}EtEtOx, and p^{RS}EtEtOx, are very similar (around 80 °C); that is, the different chirality of pEtEtOx series homopolymers, as expected, does not affect chain segment mobility (Table 2). Similarly, in the pPrMeOx series, the T_g values (around 55 °C) for p^{R}PrMeOx,

https://doi.org/10.1021/acs.macromol.2c00229
Macromolecules 2022, 55, 6176−6190

Table 2. Glass Transition Temperatures T_g of Polymers Reported Here and Compared with Literature Values for Similar Polymers

poly(2-R-4-R′-2-oxazoline)			
R =	R′ =	DP	T_g [°C]
Me	H	60	~80[59]
Me	H	35	73[57]
Me	Me	10	90[41]
Et	H	60	~60[59]
Et	Me	25	75−80[41]
Et	^{R}Et	21	82[a]
Et	^{S}Et	23	80[a]
Et	^{RS}Et	21	79[a]
Pr	H	60	~40[59]
Pr	^{R}Me	22	55[a]
Pr	^{S}Me	22	55[a]
Pr	^{RS}Me	23	56[a]
$CH_3(CH_2)_3$ (Bu)	H	60	~25[58]
$CH_3(CH_2)_4$ (Pent)	H	60	~5[59]

[a]This work, mean T_g obtained from second and third heating curve (DSC).

p^{S}PrMeOx, and p^{RS}PrMeOx are essentially identical. Clearly, the T_g of the pPrMeOx series is lower than that of pEtEtOx, which signifies higher chain segment mobility for pPrMeOx than pEtEtOx. There has been some research on the thermal properties of various POx and POzi (Table 2).[58−60] Two conclusions were drawn in this previous work: the T_g of POx decreased linearly with increasing carbon number in the side chain (from 1 to 5 carbon atoms),[59] while linear POzi have lower T_g than the POx with same side chain, which is attributable to the additional methylene unit in the main chain.[60] Previously reported p^{R}BuEtOx ([M]/[I] = 60, $T_g \approx$ 52 °C[39]) has two methylene groups more in the side chain than p^{R}EtEtOx and a T_g about 30 °C lower than the T_g of p^{R}EtEtOx ($T_g \approx$ 82 °C), which shows that with increasing number of carbon atoms in the side chain the T_g also decreases for main-chain-branched POx. Besides, the T_g of pEtEtOx is 20 °C higher than that of pEtOx, pPrMeOx has a 15 °C higher T_g than pPrOx, and the T_g of pEtEtOx is about 30 °C higher than the T_g of pPrMeOx. It should be noted that, for the 2-substituted POx, polymers with higher DP values were investigated, suggesting that at similar DPs the difference would be even more pronounced. In addition, poly(2-ethyl-4-methyl-2-oxazoline) (pEtMeOx) has a reported T_g of 75−80 °C,[41] which is basically identical with the value found here for pEtEtOx. It is apparent that the presence of an additional methylene group at the polymer backbone branch, compared to the amide side chain, significantly impedes the macromolecular segment mobility. Also, increasing the length (from C1 to C2) of the side chain branching directly from the polymer backbone does not decrease the T_g, which stands in contrast to the amide side chain. However, it would be interesting to see how the T_g evolves for longer side chains (≥C3) branching from the main chain.

Bloksma et al. investigated the enantiopure polymers p^{R}BuEtOx and p^{S}BuEtOx and racemic p^{RS}BuEtOx via XRD.[36] The enantiopure polymers were found to be semicrystalline, while the racemic polymer was amorphous. However, pEtEtOx and pPrMeOx with short side chain and main chain branches have not been investigated using XRD before. Therefore, XRD measurements were performed on the pEtEtOx and pPrMeOx series at room temperature. All the homopolymers showed broad bands (Figure S10), indicating that pEtEtOx and pPrMeOx series homopolymers are indeed amorphous, which is consistent with the absence of a T_m in the DSC measurement. The two broad bands in the XRD are in a similar position to that found previously for p^{RS}BuEtOx.[36] Generally speaking, poly(2-*n*-alkyl-2-oxazoline)s with four or more carbon atoms in the side chain are found to be semicrystalline, while the POx with one to three carbon atoms in the side chain are amorphous,[58] although crystallization has been reported for those when aqueous solutions are kept above their respective LCST.[61−63] Our data suggest that the additional carbon atoms branching off of the main chain do not promote the formation of crystalline domains in the case of POx with short side chains, although one might assume that under specific conditions crystallization might occur.

CD spectroscopy is one of the few spectroscopic techniques that is applied to analyze the secondary structure of biopolymers and synthetic polymers.[64] In 1992, Oh et al. carried out molecular mechanics calculations for pMeMeOx with DP = 20 and a corresponding tetramer.[65] The calculated structures were defined by left-handed helices containing 14 residues/3 turns with an identity period of 17.8 Å. Since then, several kinds of chiral POx have been shown to form secondary structures in solution,[37,39,41] including p^{R}EtEtOx.[38] This flexible secondary structure appears to be akin to the better-known polyproline type II helix. Accordingly, CD measurements of pEtEtOx and pPrMeOx series homopolymers were

Table 3. Physicochemical Characterization of the Triblock Copolymers Including the Yield, Molecular Weight M_n, Dispersity $Đ$, Glass Transition Temperature T_g, Extrapolated Onset Temperature of Major Mass Loss T_d, Critical Micelle Concentration CMC, and Hydrodynamic Diameter D_h

polymer	yield [%]	M_n[a] [kg mol^{-1}]	M_n[b] [kg mol^{-1}]	M_n[c] [kg mol^{-1}]	$Đ$[c]	T_g[d] [°C]	T_d[e] [°C]	CMC[f] [M·10^{-4}]	CMC[f] [g·L^{-1}]	D_h[g] [nm]
A-p^{R}EtEtOx-A	79.5	8.7	8.7	4.4	1.13	76	377	3.2	2.7	4.9 ± 1.0
A-p^{S}EtEtOx-A	62.5	8.7	8.8	4.2	1.17	76	377	3.4	3.0	4.8 ± 1.1
A-p^{RS}EtEtOx-A	76.5	8.7	8.7	4.2	1.16	77	378	3.6	3.2	4.5 ± 1.2
A-p^{R}PrMeOx-A	70.9	8.7	8.8	4.2	1.15	71	374	4.1	3.6	4.6 ± 1.2
A-p^{S}PrMeOx-A	69.3	8.7	9.1	4.1	1.15	71	373	1.2	1.1	4.7 ± 1.2
A-p^{RS}PrMeOx-A	81.9	8.7	8.8	4.2	1.18	73	380	2.2	1.9	4.9 ± 1.4

[a]According to $[M]_0/[I]_0$. [b]Obtained by ^{1}H NMR ($CDCl_3$; 300 MHz) end-group analysis evaluated as mean of all relevant signals. [c]Obtained by SEC (eluent: HFIP, calibrated with PEG standards). [d]Mean T_g obtained from second and third heating curve (DSC). [e]Onset temperature of major mass loss (TGA). [f]Obtained by pyrene assay, measured at 25 °C. [g]Mean D_h obtained by DLS from the size distribution by volume at 25 °C (polymer concentration 10 g/L in PBS, day 0).

https://doi.org/10.1021/acs.macromol.2c00229
Macromolecules 2022, 55, 6176−6190

performed between 200 and 255 nm in methanol solution (0.1 g/L) at 25 °C. A positive Cotton effect (CE) with maximum values between 210 and 220 nm was observed for the *S*-homopolymers, while a negative CE was observed for the *R*-homopolymers. This is in the wavelength range of n−π^* transition of the amide chromophore (Figure 1c and d). The opposite CE and almost symmetrical CD spectra of *R*- and *S*-homopolymers indicate that they have a similar helical conformation as proposed by Oh et al.,[65] but with opposite handedness. The racemic polymers and the 1:1 (w/w) mixtures of two corresponding chiral homopolymers did not show CEs. Besides, the CE maximum values of chiral pPrMeOx were markedly higher than that of chiral pEtEtOx, suggesting that the secondary structure formation of chiral pPrMeOx is more favorable than that of chiral pEtEtOx in methanol, which might be because of the more flexible polymer chain.

Synthesis and Characterization of ABA Triblock Copolymers. After successful homopolymer preparation, we expanded our synthetic library to the ABA triblock copolymers comprising pMeOx as hydrophilic blocks A and p^{R}EtEtOx, p^{S}EtEtOx, p^{RS}EtEtOx, p^{R}PrMeOx, p^{S}PrMeOx, and p^{RS}PrMeOx as hydrophobic blocks B. As the hydrophilic blocks A are common in all polymers, they were labeled according to their hydrophobic blocks A-p^{R}EtEtOx-A, A-p^{S}EtEtOx-A, A-p^{RS}EtEtOx-A, A-p^{R}PrMeOx-A, A-p^{S}PrMeOx-A, and A-p^{RS}PrMeOx-A, respectively. All triblock copolymers were characterized by ^{1}H NMR spectroscopy and SEC (Figures S11−S13 and Table 3). All the polymers exhibited excellent solubility in water and ethanol (solubility >200 g/L).

The same as in the case of the homopolymers, the terminal Boc moiety was used for end-group analysis by ^{1}H NMR spectroscopy (Figures S11 and S12). NMR spectra revealed a good synthetic control. The determined DPs for block A are close to 35 and for block B are close to 20, which corresponds to the respective $[M]_0/[I]_0$ values. After dialysis and lyophilization, the triblock copolymers were analyzed by SEC (Figure S13). SEC elugrams of all copolymers exhibited a narrow molar mass distribution with a reasonably low dispersity ($Đ$ < 1.2). Thermally, the ABA triblock copolymers were slightly more stable than their respective homopolymers; the extrapolated onset temperature of major mass loss was at T_d > 370 °C (compared to T_d of the homopolymers at ∼350 °C) (Figure S14, Table 3). Again, a minor weight loss step attributed to the loss of the Boc group is observed at around 220 °C. In comparison to the homopolymers, this first mass loss step is less pronounced because of the lower relative weight percentage.

The T_g values for the various triblock copolymers of the A-pEtEtOx-A and A-pPrMeOx-A series are ∼76 and ∼71 °C, respectively. No melting transition was observed in the temperature range of −50 to 190 °C. As in the case of the homopolymers, no significant differences were observed for the different stereoisomers within the A-pEtEtOx-A and A-pPrMeOx-A series. Compared to the corresponding homopolymers, the triblock copolymers containing pEtEtOx have a lower T_g, while the triblock copolymers comprising pPrMeOx blocks have a higher T_g. Obviously, no microphase separation occurs in this system under the investigated conditions, leading to one T_g value in between the T_g values of pMeOx and pEtEtOx or pPrMeOx, respectively. Similar to the situation in the homopolymers, the polymers in the A-pEtEtOx-A and A-pPrMeOx-A series exhibited a higher T_g than their structural isomers A-pPrOzi-A (T_g ≈ 50 °C) and A-pBuOx-A (T_g ≈ 62 °C).[48]

The A-pEtEtOx-A and A-pPrMeOx-A series were also characterized with XRD. No crystalline peaks were observed in diffractograms (Figure S15), confirming the amorphous character of all A-pEtEtOx-A and A-pPrMeOx-A series polymers. The chiroptical properties of the triblock copolymers were also investigated by CD in methanol (0.1 g/L) at 25 °C (Figure 2c and d). Clearly, the CD spectra of chiral triblock copolymers show a pronounced CE. The optically inactive pMeOx blocks do not prevent the secondary structures induced by the chiral block. In addition, the CE of chiral triblock copolymers in CD is also retained in aqueous solution at 25 and 50 °C (Figure S16). In contrast, as expected, the racemic triblock copolymers and the 1:1 (w/w) mixtures of two corresponding chiral triblock copolymers did not show CEs in either methanol or aqueous solution.

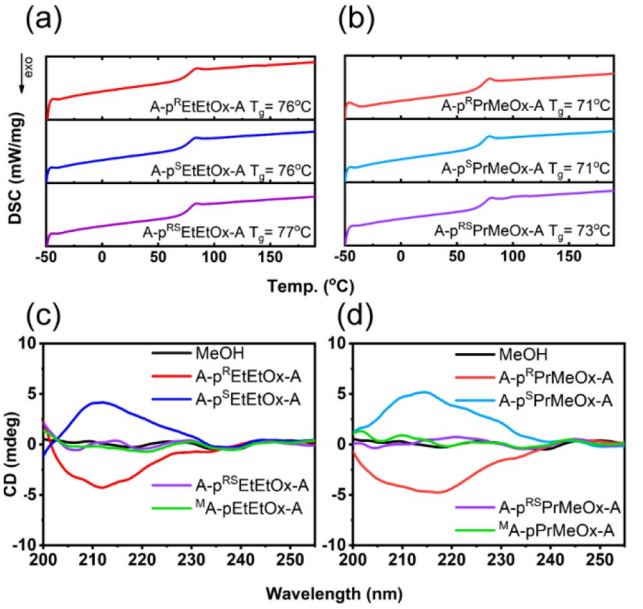

Figure 2. DSC heat flow of the third heating cycle of triblock copolymers (a) A-pEtEtOx-A and (b) A-pPrMeOx-A series. The samples were heated three times and cooled two times from −50 to 190 °C (10 °C/min). CD spectra of (c) A-pEtEtOx-A and (d) A-pPrMeOx-A series in methanol at 25 °C (polymer concentration was 0.1 g/L).

Formulation Studies. PTX is a commonly applied chemotherapeutic agent in the treatment of various cancers, such as lung, ovarian, and breast cancers.[66] CUR is a natural yellow-orange dye derived from *Curcuma longa*.[67] Because it reportedly has a plethora of biological effects such as affecting the expression of inflammatory cytokines, adhesion molecules, enzymes, the activity of several transcription factors, and their signaling pathways, CUR is considered by many as a potential treatment in cancer, atherosclerosis, neurodegenerative disease, hepatic disorders, diabetes, psoriasis, autoimmune diseases, and so on.[68] However, its chemical instability in aqueous media also prompted a very critical discussion, labeling it as a pan assay interference compound (PAIN) or invalid metabolic panacea (IMP).[69,70] While we acknowledge the importance of these issues, we also think that specifically these issues make CUR an interesting model compound for formulation studies.

https://doi.org/10.1021/acs.macromol.2c00229
Macromolecules 2022, 55, 6176−6190

Both compounds are poorly water soluble; the solubility of PTX is about 0.4−4 μg/mL,[71] while the solubility of CUR is in the range of 1−10 μg/mL,[72] depending on the polymorph. This poor solubility is one of the major issues for both compounds. Accordingly, both compounds have seen extensive efforts to improve their apparent solubility and thus, bioavailability.[73,74] Among the plethora of drug delivery systems investigated for formulation of PTX and CUR, some POx- and POzi-based formulations stand out for their extraordinary high drug loading capacity and overall solubilization for PTX and CUR.[44,48,75−77] While CUR is achiral, PTX is chiral with multiple chiral centers but, to the best of our knowledge, does not have a known enantiomer. The formulations were prepared by the thin-film hydration method. Briefly, ethanolic solutions of the polymer and drug were mixed in desired ratios, followed by ethanol removal. The resulting thin-film was dissolved by adding water (Millipore). In the resulting solution, the polymer concentration was kept at 10 g/L, while increasing the drug concentration from 1 g/L to 10 g/L in each series. The actual drug concentration achieved in the aqueous phase was assessed using HPLC or UV spectroscopy using a microplate reader after removal of nonsolubilized drug, if any, by centrifugation.

In addition to the triblock copolymers with chiral and racemic hydrophobic blocks, we also investigated 1:1 (w/w) mixtures of the chiral triblock copolymers for drug formulations. These mixtures are designated as ^{M}A-pEtEtOx-A and ^{M}A-pPrMeOx-A, respectively. The optical appearance of formulations is shown in Figure S17. The centrifuged formulations of various CUR-loaded chiral/racemic A-pEtEtOx-A and ^{M}A-pEtEtOx-A appeared homogeneous and transparent up to 4 g/L CUR feed. In contrast, a minor precipitate was observed at 6 g/L CUR feed, but the supernatant was still transparent. Interestingly, when the CUR feed increased to 8 and 10 g/L, the formulation separated to three layers: a small amount of precipitate at the bottom of the tube, an opaque layer in middle making up the majority of the sample, and a thin transparent layer on top (Figure S17a). Also extended centrifugation for 5 min (rcf = 7788 g) did not sediment the opaque layer. This seems different from a gel-like agglomerate or coacervate which was reported in the formulation of A-poly(2-(3-ethylheptyl)-2-oxazoline)-A (A-pEtHepOx-A) and CUR.[45] This behavior would be interesting to understand in more detail, but this is outside the scope of the present contribution. Here, the thin transparent layer was sampled for the measurement of CUR concentration. CUR-loaded A-pPrMeOx-A and ^{M}A-pPrMeOx-A formulations were also transparent and homogeneous at 1−4 g/L CUR feed. In contrast, at 6, 8, and 10 g/L CUR feed, there was a significant amount of precipitate with a transparent supernatant observed, with the notable exception of the formulation with A-p^{RS}PrMeOx-A at 10 g/L CUR feed. The appearance of A-p^{RS}PrMeOx-A/CUR = 10/10 (g/L) (feeding ratio) was similar to the A-pEtEtOx-A formulations at 10 g/L CUR feed and different from the A-p^{R}PrMeOx-A, A-p^{S}PrMeOx-A, and ^{M}A-pPrMeOx-A formulations at 10 g/L CUR feed.

With increasing CUR or PTX feed, the solubilized drug amount increased until it reached the maximum LC (Figure 3a−e and Table S1). At the same CUR or PTX feed, A-p^{R}EtEtOx-A, A-p^{S}EtEtOx-A, A-p^{RS}EtEtOx-A, and physical mixtures of ^{M}A-pEtEtOx-A solubilized similar amounts of CUR (Figure 3a) or PTX (Figure 3c), respectively. The

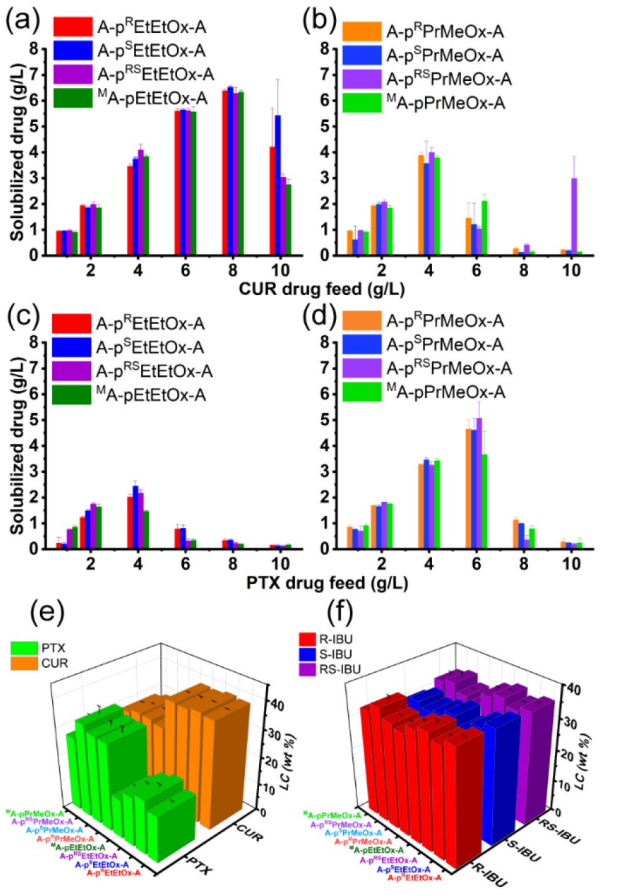

Figure 3. Solubilized CUR concentrations of CUR formulated (a) A-pEtEtOx-A and (b) A-pPrMeOx-A series with respect to the CUR feed concentration. Solubilized PTX concentrations of PTX formulated (c) A-pEtEtOx-A and (d) A-pPrMeOx-A series with respect to the PTX feed concentration. The maximum drug loading capacity of triblock copolymers and mixed polymers for (e) CUR (orange) and PTX (green) and (f) R-IBU (red), S-IBU (blue), and RS-IBU (purple). Polymer feed was 10 g/L. The data are given as means ± SD (n = 3, with the exception of A-p^{RS}PrMeOx-A/CUR = 10/10 (g/L), which is n = 5).

maximum CUR and PTX LC was found to be 39−40 wt % (6.3−6.5 g/L) and 17−20 wt % (2.0−2.4 g/L), respectively (Figure 3e). Similarly, there is relatively little difference in solubilization for CUR (Figure 3b) and PTX (Figure 3d) in the pPrMeOx series. The maximum CUR LC is 28−29 wt % (3.6−4.0 g/L), while the maximum PTX LC is 32−34 wt % (4.6−5.0 g/L) (Figure 3e). Based on these results, it seems that the chirality of the hydrophobic block in ABA triblock copolymers has no obvious effect in solubilizing CUR and PTX. There is only one major difference observed for A-p^{RS}PrMeOx-A at a CUR feed of 10 g/L (Figure 3b). This particular formulation was prepared two additional times (total of five times), confirming the extraordinarily high solubilization in this particular case. As mentioned before, the visual appearance of A-p^{RS}PrMeOx-A/CUR = 10/10 (g/L) was more similar to the A-pEtEtOx-A formulations at 10 g/L CUR feed.

Although no significant differences were observed within each polymer series, the two different platforms based on pEtEtOx and pPrMeOx obviously show a different pattern of drug loading for CUR and PTX, respectively. The polymers

https://doi.org/10.1021/acs.macromol.2c00229
Macromolecules 2022, 55, 6176−6190

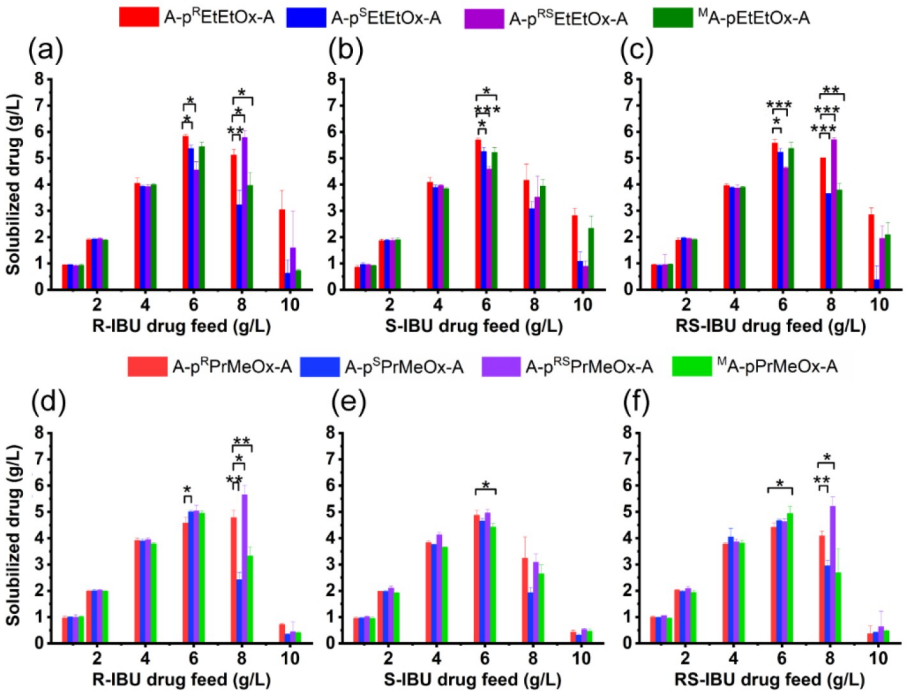

Figure 4. Solubilized (a) *R*-IBU, (b) *S*-IBU, and (c) *RS*-IBU concentrations of IBU formulated A-p^{R}EtEtOx-A (red), A-p^{S}EtEtOx-A (blue), A-p^{RS}EtEtOx-A (purple), and ^{M}A-pEtEtOx-A (green) with respect to the IBU feed concentration. Solubilized (d) *R*-IBU, (e) *S*-IBU, and (f) *RS*-IBU concentrations of IBU formulated A-p^{R}PrMeOx-A (light red), A-p^{S}PrMeOx-A (light blue), A-p^{RS}PrMeOx-A (light purple), and ^{M}A-pPrMeOx-A (light green) with respect to the IBU feed concentration. Polymer feed was 10 g/L. Data are given as means ± SD (n = 3). *p < 0.05; **p < 0.01; ***p < 0.001.

containing pEtEtOx tend to load more CUR than PTX, while the polymers containing pPrMeOx solubilize more PTX than CUR. In previous work of Lübtow et al., it was shown that even different positioning of a methylene group between the polymer side chain and the polymer main chain (comparing A-pPrOzi-A and A-pBuOx-A) can lead to a surprisingly specific drug loading for CUR and PTX, respectively.[44] Here, the difference in positioning is between the amide side chain and the backbone branch, but also leads to a similarly specific drug loading of A-pEtEtOx-A and A-pPrMeOx-A for CUR and PTX, respectively. Specifically, comparing to literature with the different isomers, the order for maximum LC for CUR is A-pPrOzi-A (≈54 wt %) > A-pEtEtOx-A (≈40 wt %) > A-pPrMeOx-A (≈29 wt %) ≥ A-pBuOx-A (≈24 wt %). In contrast, for PTX, the order for maximum LC is A-pBuOx-A (≈48%) > A-pPrMeOx-A (≈32%) > A-pPrOzi-A (≈25%) > A-pEtEtOx-A (≈18%).

IBU is a nonsteroidal anti-inflammatory drug (NSAID) and possesses a single stereogenic carbon atom, which gives rise to two enantiomers, *S*- and *R*-IBU.[78] This drug is commercially available as a racemate, even though *S*-IBU is more potent than *R*-IBU as an inhibitor of cyclo-oxygenase I.[1,79] IBU is practically insoluble in water (about 21 mg/L[80]) and has therefore often been used as a model drug to prepare formulations. Yang et al. encapsulated IBU into micelles of the copolymer brush poly(polylactide methacrylate-*co*-methacrylic acid)-*b*-poly(poly(ethylene glycol) methyl ether methacrylate) (P(PLAMA-*co*-MAA)-*b*-PPEGMA) and achieved an LC of 20.5 wt %.[81] Lehto et al. absorbed IBU into siliceous mesoporous material TUD-1 and reported an LC of 19.6 wt % after washing.[82] In addition, there are a few reports on IBU-loaded POx-based hydrogels.[83,84]

IBU is commercially available as its chiral and racemic forms, and due to its low aqueous solubility, we chose it as a model drug to study solubilization in our novel chiral and achiral POx. The series of A-pEtEtOx-A and A-pPrMeOx-A triblock copolymers were used to solubilize *R*-IBU, *S*-IBU, and *RS*-IBU.

The overview over maximum IBU LC in the resulting formulations is shown in Figure 3f and Table S2. Interestingly, both A-pEtEtOx-A and A-pPrMeOx-A series have a similar and relatively high IBU LC exceeding 30 wt %. In terms of maximum IBU LC of A-pEtEtOx-A series formulations, the highest LC is A-p^{R}EtEtOx-A/R-IBU (37 wt %) and the lowest LC is A-p^{RS}EtEtOx-A/S-IBU (32 wt %). The formulation in the A-pPrMeOx-A series with the highest LC is A-p^{RS}PrMeOx-A/R-IBU (36 wt %), and the lowest LC values are observed for A-p^{R}PrMeOx-A/RS-IBU and ^{M}A-pPrMeOx-A/S-IBU (31 wt %). The maximum LC of the rest of the formulations vary within these limits without any notable regularity. In contrast to CUR or PTX, there is no clear and significant difference for IBU solubilization between the A-pEtEtOx-A and A-pPrMeOx-A series, even though overall the A-pEtEtOx-A series seems to have somewhat higher LC values. In order to view the LC of different IBUs loaded in one of our triblock copolymers, the LC data were arranged in one coordinate system (Figure S18a–f). At up to 6 g/L IBU feed no significant differences were observed between *R*-, *S*-, and *RS*-IBU for any triblock copolymer. At 8 g/L, the LC values for *R*-IBU and *RS*-IBU are similar for the same triblock copolymer, but the LC value of *S*-IBU trails behind for several polymers, especially in A-p^{RS}EtEtOx-A and A-p^{RS}PrMeOx-A. Coincidentally, the copolymers A-p^{RS}EtEtOx-A (Figure S18c) and A-p^{RS}PrMeOx-A (Figure S18f) have the maximum LC of *R*- and *RS*-IBU at a drug feed of 8 g/L, while the others have their maximum LC at

https://doi.org/10.1021/acs.macromol.2c00229
Macromolecules 2022, 55, 6176−6190

a drug feed of 6 g/L. It is rather unexpected and remains unexplained that the two racemic polymers show the highest deviations. In contrast, at 10 g/L, again no clear or systematic difference was observed.

Besides, formulations for the different A-pEtEtOx-A (Figure 4a−c) or A-pPrMeOx-A formulations (Figure 4d−f) with different IBUs are compared. Again, up to a 4 g/L drug feed, no real difference was observed. However, with increasing the IBU feed to 6 g/L, the drug loading of A-p^{RS}EtEtOx-A was always lowest, while the drug loading for A-p^{R}EtEtOx-A was the highest in all three cases (Figure 4a−c). The drug loading for ^{M}A-pEtEtOx-A and A-p^{S}EtEtOx-A was basically the same and intermediate. At 8 g/L the picture looks much different, with the A-p^{RS}EtEtOx-A showing the highest LC values for *R*- and *RS*-IBU.

Also, for the A-pPrMeOx-A, no significant difference is observed at low feed. Different from the A-pEtEtOx-A series, the A-pPrMeOx-A series did not show a regularity of drug loading between each other at 6 g/L IBU feed. Similar to the situation at 8 g/L for A-pEtEtOx-A, the A-p^{RS}PrMeOx-A shows the highest LC values for *R*- and *RS*-IBU. To some degree, this may indicate that the solubilization of IBU is affected more by the chirality of the pEtEtOx hydrophobic block than of the pPrMeOx hydrophobic block. Besides, when the IBU feed increased to 8 g/L, the copolymers containing p^{S}EtEtOx or p^{S}PrMeOx hydrophobic blocks showed only low drug loading. Apparently, the *S*-isomer "disadvantage" discussed before for *S*-IBU also appears in A-p^{S}EtEtOx-A and A-p^{S}PrMeOx-A, but we cannot rationally explain this at the moment.

Overall, the effect of the polymer chirality of drug (chiral or achiral) solubilization was found to be minor, if existent. Considering the work of Nguyen et al.,[9] we posit that this may be due to the rather limited mobility of the polymer chains at the chiral centers. We hypothesize that the fact that the chiral centers are in the backbone, the surrounding molecules and the environment cannot properly interact with this part of the polymer; therefore the effect of the chirality beyond the secondary structure formation is minute. It would be interesting to prepare POx with chiral centers further away from the backbone or poly(2-oxazine)s with a chiral backbone, as the additional methylene ground in the backbone would create more space and flexibility of interaction of chiral centers. However, testing this hypothesis is clearly outside the scope of the present contribution.

DLS Analysis. The hydrodynamic diameters (D_h) of unloaded, CUR-loaded, and IBU-loaded polymer micelles were analyzed by DLS. It is interesting to note in this context, as determined by a pyrene assay, that both A-pEtEtOx-A and A-pPrMeOx-A series polymers exhibit a rather high CMC (1.1−3.6 g/L, i.e., 1.2−4.1 × 10^{-4} M), compared to their isomers A-pBuOx-A (8 mg/L, 1× 10^{-6} M).[46] The triblock copolymers were dissolved in PBS (polymer concentration 10 g/L), filtered (0.45 μm), and measured by DLS at 25 °C. The DLS profiles of the micelles were bi- or multimodal with broad size distributions, indicating the formation of heterogeneous particle populations (Figure S19). Comparing the size distribution by intensity, volume, and number (Figure S20), it becomes clear that for ^{M}A-pEtEtOx-A and ^{M}A-pPrMeOx-A mainly small self-assemblies (presumably micelles) of $D_h \approx 5$ nm along with very few, much larger particles (apparent $D_h \leq 250$ nm) are present. However, from these simple DLS experiments, we only obtain apparent hydrodynamic sizes based on the assumption of spherical shape. It is however not unlikely that these self-assemblies indeed have a different morphology. The other triblock copolymer solutions had a similar multimodal distribution to ^{M}A-pEtEtOx-A and ^{M}A-pPrMeOx-A. It is important to note that while they had a similar size distribution when freshly prepared, three sets of polymer solutions turned turbid after several days: ^{M}A-pPrMeOx-A solutions (10 g/L) were turbid at day 7, while A-p^{R}PrMeOx-A and A-p^{S}PrMeOx-A solutions (10 g/L) showed a slight turbidity after one month. On the contrary, A-p^{RS}PrMeOx-A and all A-pEtEtOx-A series remained transparent and retained the same particle size distribution after one month (Figure S21a). In order to investigate if the turbidity of ^{M}A-pPrMeOx-A, A-p^{R}PrMeOx-A, and A-p^{S}PrMeOx-A DLS samples was caused by crystallization, XRD measurements were performed again after freeze-drying the corresponding polymers from a cloudy water (Millipore) suspension, but no signals suggesting crystalline domains were found (Figure S22). As the chiral A-pPrMeOx-A are able to build secondary structure formation and are slightly more flexible than A-pEtEtOx-A (as evidenced by the thermal analysis), we assume that when two chiral A-pPrMeOx-A solutions were mixed to form ^{M}A-pPrMeOx-A solutions, an enantioselective aggregation happened, similar to enantioselective crystallization (but not crystallization in our case).[85] However, for the slight turbidity of A-p^{R}PrMeOx-A and A-p^{S}PrMeOx-A solutions (after one month), we have to further investigate if the secondary structure of chiral polymers is able to enhance the fusion of the micelles. Besides, the turbid DLS samples did not revert to transparency after storage at 4 °C for several days. This indicates that the turbidity of the triblock copolymer solutions is caused by self-assembly, and the thermoresponsive behavior of the hydrophobic block appears not to be sufficient to revert the self-assembly, once assembled.

The micelle size of CUR-loaded A-pEtEtOx-A and A-pPrMeOx-A series formulations was also analyzed by DLS. All the formulations (polymer/CUR = 10/2 g/L) self-assemble to form micelles with essentially the same size ($D_h \approx 25$ nm, PDI < 0.11; Table S3, Figure 5a and b). Clearly, CUR-loaded micelles exhibited a more uniform size distribution compared to the blank micelles. Dilution by 1/2 and 1/10 (v/v) samples (to 5 and 1 g/L) resulted in no change in size and distribution (data not shown). At the same time, all the CUR-loaded formulations were quite stable. The size and size distribution of formulations did not exhibit a significant change at day 7, except that of ^{M}A-pPrMeOx-A/CUR (Figure S23a and b). Here, scattering intensity is dominated by a narrow distribution of larger particles ($D_h \approx 200$ nm) after 7 days' storage, even though in terms of volume or number the distribution at $D_h \approx 25$ nm remains dominant (Figure S23c). All the formulations remained optically clear after one month, including ^{M}A-pPrMeOx-A/CUR (Figure S21b).

Similarly, *S*-IBU-loaded A-pEtEtOx-A and A-pPrMeOx-A series formulations (polymer/*S*-IBU = 10/2 (g/L)) were also studied with respect to their size distribution and dispersion stability. After thin-film hydration and filtration (0.45 μm), the maximum of the size distribution for both series of formulations lies between 10 and 20 nm (PDI < 0.23, Table S4, Figure 5c and d) with A-p^{R}EtEtOx-A, ^{M}A-pEtEtOx-A, and ^{M}A-pPrMeOx-A showing somewhat broader distributions. The higher PDI values are primarily due to a minor population at larger sizes, in particular for A-p^{R}EtEtOx-A. Obviously, the formulations of the chiral compound S-IBU are quite similar

https://doi.org/10.1021/acs.macromol.2c00229
Macromolecules 2022, 55, 6176−6190

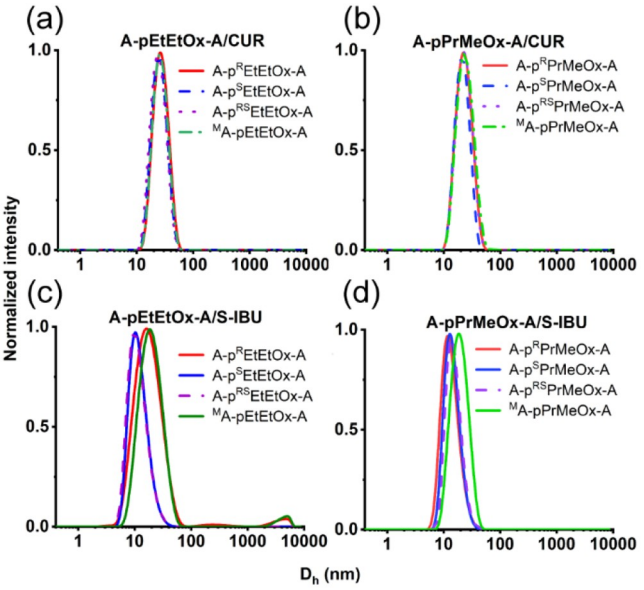

Figure 5. Size distribution by intensity of (a) A-pEtEtOx-A/CUR, (b) A-pPrMeOx-A/CUR, (c) A-pEtEtOx-A/S-IBU, and (d) A-pPrMeOx-A/S-IBU formulations 10/2 (g/L) in PBS at day 0. The samples were measured at 25 °C after filtration using a 0.45 μm PVDF syringe filter.

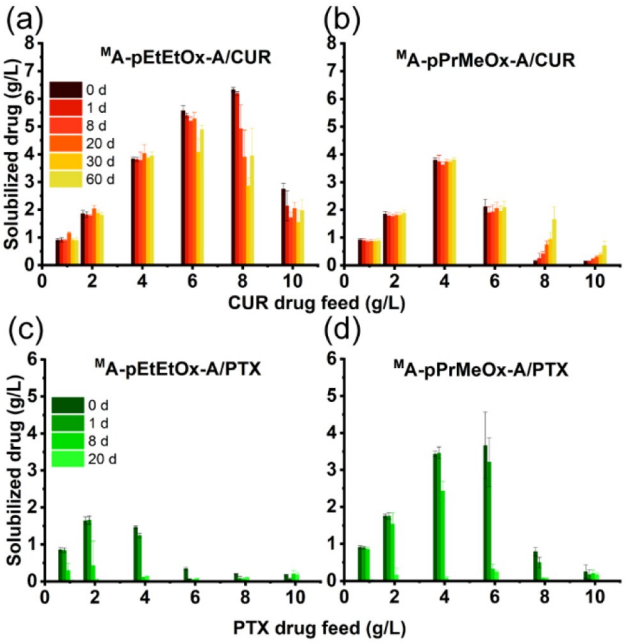

Figure 6. Long-term stability of CUR-loaded (a) physical mixture ^{M}A-pEtEtOx-A and (b) physical mixture ^{M}A-pPrMeOx-A formulationwith respect to with respect to CUR feed concentration (polymer feed 10 g/L, CUR feed 1−10 g/L, 0−60 d). Long-term stability of PTX-loaded (c) physical mixture ^{M}A-pEtEtOx-A and (d) physical mixture ^{M}A-pPrMeOx-A formulation with respect to PTX feed concentration (polymer feed 10 g/L, PTX feed 1−10 g/L, 0−20 d). Data are given as means ± SD (n = 3).

but appear less uniform compared to the curcumin formulations; however, no clear trend between the different chiralities can be seen at day 0. After 7 days' storage, the formulations remain transparent and their size and size distribution appear now more uniform, except ^{M}A-pPrMeOx-A/S-IBU (Figure S24a and b). This formulation turned turbid, similar to the plain ^{M}A-pPrMeOx-A solution (Figure S21c and Figure S24c), but different from the ^{M}A-pPrMeOx-A/CUR formulation. Also after one month, the other *S*-IBU-loaded formulations remained transparent.

Long-Term Stability Studies of the Formulations. In order to investigate the potential shelf life of the formulations (A-pEtEtOx-A and A-pPrMeOx-A series), the freshly prepared CUR, PTX, and IBU aqueous formulations were stored at ambient conditions containing the initial precipitate after thin-film hydration (if any). The samples were collected at day 0, 1, 8, 20, 30, and 60 with centrifugation before each collection to sediment the precipitate (if any). The soluble drug remaining in the supernatant was then quantified.

In each polymer series (A-pEtEtOx-A and A-pPrMeOx-A), the stability of most formulations follows a certain pattern. Exemplarily, CUR-loaded ^{M}A-pEtEtOx-A and ^{M}A-pPrMeOx-A formulations are shown in Figure 6a,b. The formulations with a CUR feed of 1−8 g/L were relatively stable up to 24 h; less than 1 wt % loss in the LC was observed in both the ^{M}A-pEtEtOx-A and ^{M}A-pPrMeOx-A formulations. In the case of ^{M}A-pEtEtOx-A formulations (Figure 6a), at up to 4 g/L CUR feed, no reduction in drug loading was observed even after 60 days. In contrast, at 6 g/L CUR feed and above, a moderate and gradual decrease in LC was observed. Overall, the A-pPrMeOx-A formulations series behaves differently compared to the A-pEtEtOx-A series, but within the series all formulations behave very similarly, with the notable exception of A-p^{RS}PrMeOx-A at 10 g/L CUR feed (*vide infra*). At up to a CUR feed of 6 g/L, all formulations are very stable for 60 days (Figure 6b). However, at a CUR feed of 8 and 10 g/L, the concentration of CUR found in the supernatant increased gradually and quite significantly. For instance, at 8 g/L CUR feed ^{M}A-pPrMeOx-A formulation, a 10-fold increase in the drug loading (0.16 ± 0.04 g/L (day 0) to 1.66 ± 0.45 g/L (day 60)) was observed. Previously, a similar phenomenon was also reported for POx/POzi micelles with a moderately hydrophobic block, such as in the CUR-loaded A-pBuOx-A formulation (CUR feed ≥5 g/L)[48] and CUR-loaded A-EtHepOx-A formulation (CUR feed 2−10 g/L).[45] It is speculated that an initially formed drug/polymer coacervate redissolves over time, probably via an internal reorganization in the polymer drug self-assembly.[45,86] Such a time-dependent change in the self-assembly of nanoformulations and its effect on the biodistribution and pharmacological performance has been recently reported by Kabanov.[86]

The formulation of A-p^{RS}PrMeOx-A/CUR at 10 g/L CUR feed showed a very different behavior, exhibiting a rather high drug loading at day 0 (23 wt %, Figure 3b), followed by an initial small decrease and a subsequent stronger increase leading to an LC = 32 wt % at day 60 (Figure S25). At this point, we cannot explain this behavior satisfyingly.

The long-term stability of PTX-loaded ^{M}A-pEtEtOx-A and ^{M}A-pPrMeOx-A formulations was also studied. The maximum PTX-loaded ^{M}A-pEtEtOx-A formulation (2 g/L PTX feed) was quite stable up to 24 h (Figure 6c). Afterward, the PTX LC dropped rapidly from 14 wt % (day 1) to 6 wt % (day 8). At a PTX feed of 4 g/L, a minor loss (i.e., 2 wt %) in the LC was observed after 24 h; then the LC dramatically dropped to 1 wt % (day 8). At day 20, less than 3 wt % PTX was left in the supernatant of all ^{M}A-pEtEtOx-A/PTX formulations. In comparison, the PTX-loaded ^{M}A-pPrMeOx-A formulations were relatively stable at 4 g/L PTX feed, as no LC reduction

https://doi.org/10.1021/acs.macromol.2c00229
Macromolecules 2022, 55, 6176−6190

was observed at 24 h (Figure 6d), while at 6 g/L PTX feed, ^{M}A-pPrMeOx-A formulation showed a 3 wt % LC loss at 24 h. However, the PTX-loaded ^{M}A-pPrMeOx-A formulation was also not stable for more days. After 8 days' storage, the LC of 4 g/L PTX feed decreased from 26 wt % (day 1) to 20 wt % (day 8), and the 6 g/L PTX feed decreased from 24 wt % (day 1) to 3 wt % (day 8). The PTX LC was less than 3 wt % in all ^{M}A-pPrMeOx-A/PTX formulations at day 20.

Generally, the chirality of copolymers does not appear to affect the long-term stability of the IBU-loaded formulation, with the notable exception of a few A-p^{RS}EtEtOx-A and A-p^{RS}PrMeOx-A formulations (*vide infra*). Exemplarily, the long-term stability of ^{M}A-pEtEtOx-A/RS-IBU and ^{M}A-pPrMeOx-A/RS-IBU formulations is used to discuss the general behavior of A-pEtEtOx-A and A-pPrMeOx-A series formulations, respectively (Figure 7a,b). At up to 6 g/L RS-IBU feed, the LC of ^{M}A-pEtEtOx-A/RS-IBU decreased slowly in 30 days. In contrast, at 8 and 10 g/L RS-IBU feed, the LC dropped significantly around day 20 (Figure 7a). Comparing to A-pEtEtOx-A series, the IBU-loaded A-pPrMeOx-A formulations appeared to be a relatively more stable formulation. The LC of ^{M}A-pPrMeOx-A/RS-IBU decreased evenly and relatively slowly over 60 days, irrespective of the RS-IBU feed (Figure 7b). At day 60, only 7 wt % LC loss was observed at 6 g/L RS-IBU feed.

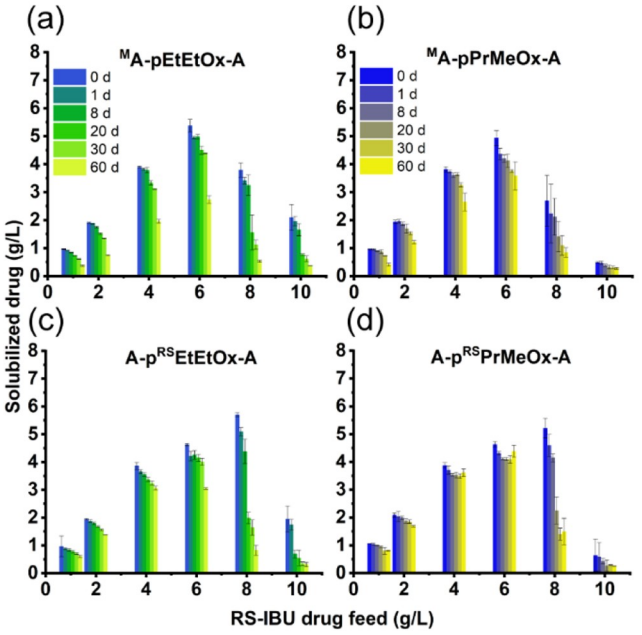

Figure 7. Long-term stability of RS-IBU-loaded (a) physical mixture of ^{M}A-pEtEtOx-A, (b) physical mixture ^{M}A-pPrMeOx-A, (c) A-p^{RS}EtEtOx-A and (d) A-p^{RS}PrMeOx-A formulation with respect to RS-IBU feed concentration (polymer feed 10 g/L, RS-IBU feed 1−10 g/L). Data are given as means ± SD (n = 3).

As mentioned in the drug-loading part, A-p^{RS}EtEtOx-A and A-p^{RS}PrMeOx-A have the maximum LC of *R*- and *RS*-IBU at a drug feed of 8 g/L. Accordingly, the long-term stability of RS-IBU-loaded A-p^{RS}EtEtOx-A and A-p^{RS}PrMeOx-A formulations is shown for these special cases (Figure 7c and d). Similar to ^{M}A-pEtEtOx-A/RS-IBU, at up to 6 g/L RS-IBU feed, the LC of A-p^{RS}EtEtOx-A/RS-IBU decreased gradually over a 30-day period. However, at 8 g/L RS-IBU feed, formulations were not very stable, as within 24 h, a 6 wt % LC loss was observed (Figure 7c). Finally, the LC of the 8 g/L RS-IBU feed A-p^{RS}EtEtOx-A/RS-IBU formulation dropped to the same level of ^{M}A-pEtEtOx-A/RS-IBU after 60 days. Similarly, the A-p^{RS}PrMeOx-A/RS-IBU formulations were relatively stable for 60 days at 6 g/L RS-IBU feed (Figure 7d). In contrast, at 8 g/L RS-IBU feed, the stability was compromised.

CONCLUSION

In summary, we have synthesized two series of novel chiral and racemic homopolymer poly(2,4-disubstituted-2-oxazoline)s via LCROP, pEtEtOx and pPrMeOx series. Subsequently, novel ABA triblock copolymers were synthesized using these hydrophobic pEtEtOx and pPrMeOx as block B and hydrophilic pMeOx as block A. Attributable to the steric hindrance caused by the methyl/ethyl group on the polymer backbone, both pEtEtOx and pPrMeOx series show less chain flexibility than pEtOx and pPrOx, respectively; otherwise, the thermal properties of homopolymers within each series are similar. These chiral homopolymers and triblock copolymers (including chiral central block) are able to form secondary structure in solution, as evidenced by CD spectroscopy. Both A-pEtEtOx-A and A-pPrMeOx-A series copolymers formed rather heterogeneous self-assemblies in aqueous solution.

The drug formulations based on the triblock copolymers and drugs CUR, PTX, and IBU (chiral and racemic) were prepared through the thin-film method. The difference in drug solubilization between chiral and racemic triblock copolymers and the 1:1 (w/w) mixtures of two corresponding chiral copolymers is not significant for either CUR or PTX in most cases. However, we found that shifting a methylene group from the N-substituted side chain to the backbone branch does lead to differences in drug loading between A-pEtEtOx-A and A-pPrMeOx-A, similar to the isomeric pair of A-pBuOx-A and A-pPrOzi-A. As for the IBU, the chirality of triblock copolymers appears to affect the LC only at high drug feed (IBU 8 g/L and above, polymer 10 g/L). The LCs of A-p^{S}EtEtOx-A and A-p^{S}PrMeOx-A are noticeably lower than their *R*- and *RS*-isomers. The origins for the observed, albeit small differences for chiral POx require further investigations; in particular the influence on interactions with biological systems will be a matter for future investigations.

ASSOCIATED CONTENT

Supporting Information

The Supporting Information is available free of charge at https://pubs.acs.org/doi/10.1021/acs.macromol.2c00229.

NMR spectra (^{1}H and ^{13}C NMR); SEC elugrams; TGA; XRD patterns; CD spectra (in water solution); graph of drug solubility; data of maximum LC and LE; DLS; optical appearance of selected formulations; long-term stability of A-p^{RS}PrMeOx-A/CUR (10/10 g/L) (PDF)

AUTHOR INFORMATION

Corresponding Author

Robert Luxenhofer − *Functional Polymer Materials, Chair for Chemical Technology of Material Synthesis, Institute for Functional Materials and Biofabrication, Department of Chemistry and Pharmacy, Julius-Maximilians-University Würzburg, 97070 Würzburg, Germany; Soft Matter Chemistry, Department of Chemistry and Helsinki Institute of*

https://doi.org/10.1021/acs.macromol.2c00229
Macromolecules 2022, 55, 6176−6190

Sustainability Science, Faculty of Science, University of Helsinki, 00014 Helsinki, Finland; orcid.org/0000-0001-5567-7404; Email: robert.luxenhofer@helsinki.fi

Authors

Mengshi Yang − *Functional Polymer Materials, Chair for Chemical Technology of Material Synthesis, Institute for Functional Materials and Biofabrication, Department of Chemistry and Pharmacy, Julius-Maximilians-University Würzburg, 97070 Würzburg, Germany*

Malik Salman Haider − *Functional Polymer Materials, Chair for Chemical Technology of Material Synthesis, Institute for Functional Materials and Biofabrication, Department of Chemistry and Pharmacy, Julius-Maximilians-University Würzburg, 97070 Würzburg, Germany*

Stefan Forster − *Functional Polymer Materials, Chair for Chemical Technology of Material Synthesis, Institute for Functional Materials and Biofabrication, Department of Chemistry and Pharmacy, Julius-Maximilians-University Würzburg, 97070 Würzburg, Germany*

Chen Hu − *Functional Polymer Materials, Chair for Chemical Technology of Material Synthesis, Institute for Functional Materials and Biofabrication, Department of Chemistry and Pharmacy, Julius-Maximilians-University Würzburg, 97070 Würzburg, Germany*

Complete contact information is available at: https://pubs.acs.org/10.1021/acs.macromol.2c00229

Notes

The authors declare no competing financial interest.

■ ACKNOWLEDGMENTS

This work was supported by the Deutsche Forschungsgemeinschaft, project #398461692 (awarded to R.L.). Moreover, M.Y., C.H., and M.S.H. are grateful to the China Scholarship Council (CSC) and higher education commission of Pakistan-German academic exchange services (HEC-DAAD Pakistan), respectively, for a doctoral fellowship. M.Y. is also grateful for financial support through an DAAD STIBET scholarship offered by the German Academic Exchange Service (DAAD), financed by the German Federal Foreigh Office (AA). We also thank the Department for Functional Materials in Medicine and Dentistry (Julius-Maximilians-University of Würzburg) for instrument access and Prof. Paul D. Dalton and Prof. Dirk Kurth for valuable discussions.

■ REFERENCES

(1) Nguyen, L. A.; He, H.; Pham-Huy, C. Chiral Drugs: An Overview. *Int. J. Biomed. Sci.* **2006**, *2* (2), 85−100.

(2) Hirose, D.; Isobe, A.; Quiñoá, E.; Freire, F.; Maeda, K. Three-state switchable chiral stationary phase based on helicity control of an optically active poly (phenylacetylene) derivative by using metal cations in the solid state. *J. Am. Chem. Soc.* **2019**, *141* (21), 8592−8598.

(3) Abyaneh, H. S.; Vakili, M. R.; Lavasanifar, A. The effect of polymerization method in stereo-active block copolymers on the stability of polymeric micelles and their drug release profile. *Pharm. Res.* **2014**, *31* (6), 1485−1500.

(4) Mochida, Y.; Cabral, H.; Miura, Y.; Albertini, F.; Fukushima, S.; Osada, K.; Nishiyama, N.; Kataoka, K. Bundled assembly of helical nanostructures in polymeric micelles loaded with platinum drugs enhancing therapeutic efficiency against pancreatic tumor. *ACS Nano* **2014**, *8* (7), 6724−6738.

(5) Ding, J.; Li, C.; Zhang, Y.; Xu, W.; Wang, J.; Chen, X. Chirality-mediated polypeptide micelles for regulated drug delivery. *Acta biomaterialia* **2015**, *11*, 346−355.

(6) Abyaneh, H. S.; Vakili, M. R.; Shafaati, A.; Lavasanifar, A. Block Copolymer Stereoregularity and Its Impact on Polymeric Micellar Nanodrug Delivery. *Mol. Pharmaceutics* **2017**, *14* (8), 2487−2502.

(7) Feng, K.; Wang, S. Z.; Ma, H. R.; Chen, Y. J. Chirality plays critical roles in enhancing the aqueous solubility of nocathiacin I by block copolymer micelles. *J. Pharm. Pharmacol.* **2012**, *65* (1), 64−71.

(8) Hu, J. L.; Tang, J. H.; Qiu, X. Y.; Han, Y. D.; Liu, Q.; Chen, X. S.; Jing, X. B. Effects of stereoregularity of multiblock copoly(rac-lactide)s on stereocomplex microparticles and their insulin delivery. *Macromol. Biosci.* **2005**, *5* (12), 1193−1199.

(9) Nguyen, H. V. T.; Jiang, Y.; Mohapatra, S.; Wang, W.; Barnes, J. C.; Oldenhuis, N. J.; Chen, K. K.; Axelrod, S.; Huang, Z.; Chen, Q.; Golder, M. R.; Young, K.; Suvlu, D.; Shen, Y.; Willard, A. P.; Hore, M. J. A.; Gómez-Bombarelli, R.; Johnson, J. A. Bottlebrush polymers with flexible enantiomeric side chains display differential biological properties. *Nat. Chem.* **2022**, *14* (1), 85−93.

(10) Luxenhofer, R.; Han, Y. C.; Schulz, A.; Tong, J.; He, Z. J.; Kabanov, A. V.; Jordan, R. Poly(2-oxazoline)s as Polymer Therapeutics. *Macromol. Rapid Commun.* **2012**, *33* (19), 1613−1631.

(11) Lorson, T.; Lübtow, M. M.; Wegener, E.; Haider, M. S.; Borova, S.; Nahm, D.; Jordan, R.; Sokolski-Papkov, M.; Kabanov, A. V.; Luxenhofer, R. Poly(2-oxazoline)s based biomaterials: A comprehensive and critical update. *Biomaterials* **2018**, *178*, 204−280.

(12) Witte, H.; Seeliger, W. Cyclische Imidsäureester aus Nitrilen und Aminoalkoholen. *Liebigs Ann. Chem.* **1974**, *1974*, 996−1009.

(13) Seeliger, W.; Aufderhaar, E.; Diepers, W.; Feinauer, R.; Nehring, R.; Thier, W.; Hellmann, H. Neuere Synthesen und Reaktionen cyclischer Imidsaeureester. *Angew. Chem.* **1966**, *78* (20), 913−927.

(14) Hansen, J. F.; Cooper, C. S. Preparation and alkylation of a new chiral oxazoline from L-serine. *J. Org. Chem.* **1976**, *41* (19), 3219−3220.

(15) Rossegger, E.; Schenk, V.; Wiesbrock, F. Design strategies for functionalized poly (2-oxazoline) s and derived materials. *Polymers* **2013**, *5* (3), 956−1011.

(16) Bodner, T.; Ellmaier, L.; Schenk, V.; Albering, J.; Wiesbrock, F. Delocalized π-electrons in 2-oxazoline rings resulting in negatively charged nitrogen atoms: revealing the selectivity during the initiation of cationic ring-opening polymerizations. *Polym. Int.* **2011**, *60* (8), 1173−1179.

(17) Glassner, M.; Vergaelen, M.; Hoogenboom, R. Poly (2-oxazoline) s: A comprehensive overview of polymer structures and their physical properties. *Polym. Int.* **2018**, *67* (1), 32−45.

(18) Zalipsky, S.; Hansen, C. B.; Oaks, J. M.; Allen, T. M. Evaluation of blood clearance rates and biodistribution of poly (2-oxazoline)-grafted liposomes. *J. Pharm. Sci.* **1996**, *85* (2), 133−137.

(19) Woodle, M. C.; Engbers, C. M.; Zalipsky, S. New amphipatic polymer-lipid conjugates forming long-circulating reticuloendothelial system-evading liposomes. *Bioconjugate Chem.* **1994**, *5* (6), 493−496.

(20) Konradi, R.; Pidhatika, B.; Mühlebach, A.; Textor, M. Poly-2-methyl-2-oxazoline: a peptide-like polymer for protein-repellent surfaces. *Langmuir* **2008**, *24* (3), 613−616.

(21) Zhang, N.; Pompe, T.; Amin, I.; Luxenhofer, R.; Werner, C.; Jordan, R. Tailored Poly(2-oxazoline) Polymer Brushes to Control Protein Adsorption and Cell Adhesion. *Macromol. Biosci.* **2012**, *12* (7), 926−936.

(22) Knop, K.; Hoogenboom, R.; Fischer, D.; Schubert, U. S. Poly (ethylene glycol) in drug delivery: pros and cons as well as potential alternatives. *Angew. Chem., Int. Ed.* **2010**, *49* (36), 6288−6308.

(23) Barz, M.; Luxenhofer, R.; Zentel, R.; Vicent, M. J. Overcoming the PEG-addiction: well-defined alternatives to PEG, from structure−property relationships to better defined therapeutics. *Polym. Chem.* **2011**, *2* (9), 1900−1918.

(24) Grube, M.; Leiske, M. N.; Schubert, U. S.; Nischang, I. POx as an alternative to PEG? A hydrodynamic and light scattering study. *Macromolecules* **2018**, *51* (5), 1905−1916.

(25) Pidhatika, B.; Möller, J.; Vogel, V.; Konradi, R. Nonfouling surface coatings based on poly (2-methyl-2-oxazoline). *Chimia* **2008**, *62* (4), 264−269.
(26) Mansfield, E. D.; Victor, R.; Kowalczyk, R. M.; Grillo, I.; Hoogenboom, R.; Sillence, K.; Hole, P.; Williams, A. C.; Khutoryanskiy, V. V. Side chain variations radically alter the diffusion of poly (2-alkyl-2-oxazoline) functionalised nanoparticles through a mucosal barrier. *Biomater. Sci.* **2016**, *4* (9), 1318−1327.
(27) Luxenhofer, R.; Sahay, G.; Schulz, A.; Alakhova, D.; Bronich, T. K.; Jordan, R.; Kabanov, A. V. Structure-property relationship in cytotoxicity and cell uptake of poly(2-oxazoline) amphiphiles. *J. Controlled Release* **2011**, *153* (1), 73−82.
(28) Schmitz, M.; Kuhlmann, M.; Reimann, O.; Hackenberger, C. P.; Groll, J. Side-chain cysteine-functionalized poly (2-oxazoline) s for multiple peptide conjugation by native chemical ligation. *Biomacromolecules* **2015**, *16* (4), 1088−1094.
(29) Luxenhofer, R.; López-García, M.; Frank, A.; Kessler, H.; Jordan, R. First poly (2-oxazoline)-peptide conjugate for targeted radionuclide cancer therapy. *PMSE Prepr* **2006**, *95*, 283−284.
(30) Tong, J.; Luxenhofer, R.; Yi, X. A.; Jordan, R.; Kabanov, A. V. Protein Modification with Amphiphilic Block Copoly(2-oxazoline)s as a New Platform for Enhanced Cellular Delivery. *Mol. Pharmaceutics* **2010**, *7* (4), 984−992.
(31) Oudin, A.; Chauvin, J.; Gibot, L.; Rols, M.-P.; Balor, S.; Goudounèche, D.; Payré, B.; Lonetti, B.; Vicendo, P.; Mingotaud, A.-F. Amphiphilic polymers based on polyoxazoline as relevant nanovectors for photodynamic therapy. *J. Mater. Chem. B* **2019**, *7* (32), 4973−4982.
(32) Waschinski, C. J.; Tiller, J. C. Poly (oxazoline) s with telechelic antimicrobial functions. *Biomacromolecules* **2005**, *6* (1), 235−243.
(33) Aoi, K.; Okada, M. Polymerization of oxazolines. *Prog. Polym. Sci.* **1996**, *21* (1), 151−208.
(34) Saegusa, T.; Kobayash, S.; Ishiguro, M. New Route to optically-active linear poly(propylenimine). *Macromolecules* **1974**, *7* (6), 958−959.
(35) Saegusa, T.; Hirao, T.; Ito, Y. Polymerization of (4S, 5R)-4-Carbomethoxy-5-methyl-2-oxazoline. *Macromolecules* **1975**, *8* (1), 87−87.
(36) Bloksma, M. M.; Hendrix, M.; Schubert, U. S.; Hoogenboom, R. Ordered Chiral Structures in the Crystals of Main-Chain Chiral Poly(2-oxazoline)s. *Macromolecules* **2010**, *43* (10), 4654−4659.
(37) Bloksma, M. M.; Rogers, S.; Schubert, U. S.; Hoogenboom, R. Secondary structure formation of main-chain chiral poly(2-oxazoline)-s in solution. *Soft Matter* **2010**, *6* (5), 994−1003.
(38) Bloksma, M. M.; Rogers, S.; Schubert, U. S.; Hoogenboom, R. Main-Chain Chiral Poly(2-oxazoline)s: Influence of Alkyl Side-chain on Secondary Structure Formation in Solution. *J. Polym. Sci., Polym. Chem.* **2011**, *49* (13), 2790−2801.
(39) Bloksma, M. M.; Schubert, U. S.; Hoogenboom, R. Main-chain chiral copoly(2-oxazoline)s. *Polym. Chem.* **2011**, *2* (1), 203−208.
(40) Bloksma, M. M.; Hoeppener, S.; D'Haese, C.; Kempe, K.; Mansfeld, U.; Paulus, R. M.; Gohy, J. F.; Schubert, U. S.; Hoogenboom, R. Self-assembly of chiral block and gradient copolymers. *Soft Matter* **2012**, *8* (1), 165−172.
(41) Luxenhofer, R.; Huber, S.; Hytry, J.; Tong, J.; Kabanov, A. V.; Jordan, R. Chiral and Water-Soluble Poly(2-oxazoline)s. *J. Polym. Sci., Polym. Chem.* **2013**, *51* (3), 732−738.
(42) Bott, K.; Schmidt, P. Neue, optisch aktive Polymere für die chromatographische Racemattrennung, European Patent. DE3418525A1;EP0161547A2;EP0161547A3;EP0161547B1, 1985.
(43) Seo, Y.; Schulz, A.; Han, Y. C.; He, Z. J.; Bludau, H.; Wan, X. M.; Tong, J.; Bronich, T. K.; Sokolsky, M.; Luxenhofer, R.; Jordan, R.; Kabanov, A. V. Poly(2-oxazoline) block copolymer based formulations of taxanes: effect of copolymer and drug structure, concentration, and environmental factors. *Polym. Adv. Technol.* **2015**, *26* (7), 837−850.
(44) Lübtow, M. M.; Hahn, L.; Haider, M. S.; Luxenhofer, R. Drug Specificity, Synergy and Antagonism in Ultrahigh Capacity Poly(2-oxazoline)/Poly(2-oxazine) based Formulations. *J. Am. Chem. Soc.* **2017**, *139* (32), 10980−10983.
(45) Lübtow, M. M.; Kessler, L.; Appelt-Menzel, A.; Lorson, T.; Gangloff, N.; Kirsch, M.; Dahms, S.; Luxenhofer, R. More Is Sometimes Less: Curcumin and Paclitaxel Formulations Using Poly(2-oxazoline) and Poly(2-oxazine)-Based Amphiphiles Bearing Linear and Branched C9 Side Chains. *Macromol. Biosci.* **2018**, *18* (11), 1800155.
(46) Lübtow, M. M.; Haider, M. S.; Kirsch, M.; Klisch, S.; Luxenhofer, R. Like Dissolves Like? A Comprehensive Evaluation of Partial Solubility Parameters to Predict Polymer-Drug Compatibility in Ultrahigh Drug-Loaded Polymer Micelles. *Biomacromolecules* **2019**, *20* (8), 3041−3056.
(47) Kalyanasundaram, K.; Thomas, J. K. Environmental effects on vibronic band intensities in pyrene monomer fluorescence and their application in studies of micellar systems. *J. Am. Chem. Soc.* **1977**, *99* (7), 2039−2044.
(48) Lübtow, M. M.; Nelke, L. C.; Seifert, J.; Kuhnemundt, J.; Sahay, G.; Dandekar, G.; Nietzer, S. L.; Luxenhofer, R. Drug induced micellization into ultra-high capacity and stable curcumin nano-formulations: Physico-chemical characterization and evaluation in 2D and 3D in vitro models. *J. Controlled Release* **2019**, *303*, 162−180.
(49) Sarp, G.; Yilmaz, E. A flower-like hybrid material composed of Fe_3O_4, graphene oxide and CdSe nanodots for magnetic solid phase extraction of ibuprofen prior to its quantification by HPLC detection. *Microchim. Acta* **2019**, *186* (11), 744.
(50) Magiera, S.; Piwowarczyk, A.; Wegrzyn, A. A study of the enantiospecific degradation of ibuprofen in model aqueous samples using LLME-HPLC- DAD. *Anal. Methods* **2016**, *8* (43), 7789−7799.
(51) Ingram, M. J.; Moynihan, H. A.; Powell, M. W.; Rostron, C. Synthesis and hydrolytic behaviour of glycerol-1,.2-diibuprofenate-3-nitrate, a putative pro-drug of ibuprofen and glycerol-1-nitrate. *J. Pharm. Pharmacol.* **2010**, *53* (3), 345−350.
(52) Hoogenboom, R.; Schlaad, H. Thermoresponsive poly (2-oxazoline) s, polypeptoids, and polypeptides. *Polym. Chem.* **2017**, *8* (1), 24−40.
(53) Lorson, T.; Jaksch, S.; Lübtow, M. M.; Jungst, T.; Groll, J.; Luhmann, T.; Luxenhofer, R. A Thermogelling Supramolecular Hydrogel with Sponge-Like Morphology as a Cytocompatible Bioink. *Biomacromolecules* **2017**, *18* (7), 2161−2171.
(54) Bloksma, M. M.; Paulus, R. M.; van Kuringen, H. P. C.; van der Woerdt, F.; Lambermont-Thijs, H. M. L.; Schubert, U. S.; Hoogenboom, R. Thermoresponsive Poly(2-oxazine)s. *Macromol. Rapid Commun.* **2012**, *33* (1), 92−96.
(55) Warne, N. M.; Finnegan, J. R.; Feeney, O. M.; Kempe, K. Using 2-isopropyl-2-oxazine to explore the effect of monomer distribution and polymer architecture on the thermoresponsive behavior of copolymers. *J. Polym. Sci.* **2021**, *59* (22), 2783−2796.
(56) Jing, C.; Suzuki, Y.; Matsumoto, A. Thermal decomposition of methacrylate polymers containing tert-butoxycarbonyl moiety. *Polym. Degrad. Stab.* **2019**, *166*, 145−154.
(57) Haider, M. S.; Lübtow, M. M.; Endres, S.; Forster, S.; Flegler, V. J.; Böttcher, B.; Aseyev, V. O.; Pöppler, A.-C.; Luxenhofer, R. Think beyond the core: The impact of the hydrophilic corona on the drug solubilization using polymer micelles. *ACS Appl. Mater. Interfaces* **2020**, *12* (22), 24531−24543.
(58) Rettler, E. F. J.; Kranenburg, J. M.; Lambermont-Thijs, H. M.; Hoogenboom, R.; Schubert, U. S. Thermal, Mechanical, and Surface Properties of Poly (2-N-alkyl-2-oxazoline) s. *Macromol. Chem. Phys.* **2010**, *211* (22), 2443−2448.
(59) Hoogenboom, R.; Fijten, M. W. M.; Thijs, H. M. L.; Van Lankvelt, B. M.; Schubert, U. S. Microwave-assisted synthesis and properties of a series of poly(2-alkyl-2-oxazoline)s. *Des. Monomers Polym.* **2005**, *8* (6), 659−671.
(60) Bloksma, M. M.; Schubert, U. S.; Hoogenboom, R. Poly(cyclic imino ether)s Beyond 2-Substituted-2-oxazolines. *Macromol. Rapid Commun.* **2011**, *32* (18), 1419−1441.

https://doi.org/10.1021/acs.macromol.2c00229
Macromolecules 2022, 55, 6176−6190

(61) Demirel, A. L.; Meyer, M.; Schlaad, H. Formation of polyamide nanofibers by directional crystallization in aqueous solution. *Angew. Chem.* **2007**, *119* (45), 8776−8778.
(62) Obeid, R.; Tanaka, F.; Winnik, F. M. Heat-induced phase transition and crystallization of hydrophobically end-capped poly (2-isopropyl-2-oxazoline) s in water. *Macromolecules* **2009**, *42* (15), 5818−5828.
(63) Güner, P. T.; Miko, A.; Schweinberger, F. F.; Demirel, A. L. Self-assembled poly (2-ethyl-2-oxazoline) fibers in aqueous solutions. *Polym. Chem.* **2012**, *3* (2), 322−324.
(64) Eliel, E. L.; Wilen, S. H. *Stereochemistry of Organic Compounds*; John Wiley & Sons, 1994.
(65) Oh, Y. S.; Yamazaki, T.; Goodman, M. Syntheses and circular dichroism (CD) spectra of optically active polyoxazolines and their model compounds. *Macromolecules* **1992**, *25* (23), 6322−6331.
(66) Jordan, M. A.; Wilson, L. Microtubules as a target for anticancer drugs. *Nat. Rev. Cancer* **2004**, *4* (4), 253−265.
(67) Aggarwal, B. B.; Kumar, A.; Bharti, A. C. Anticancer potential of curcumin: preclinical and clinical studies. *Anticancer Res.* **2003**, *23* (1/A), 363−398.
(68) Das, U. N. Molecular Mechanisms of Action of Curcumin and Its Relevance to Some Clinical Conditions. In *Curcumin for Neurological and Psychiatric Disorders*; Elsevier, 2019; pp 325−332.
(69) Baell, J.; Walters, M. A. Chemistry: Chemical con artists foil drug discovery. *Nature News* **2014**, *513* (7519), 481.
(70) Baell, J. B. Feeling nature's PAINS: natural products, natural product drugs, and pan assay interference compounds (PAINS). *J. Nat. Prod.* **2016**, *79* (3), 616−628.
(71) Ma, P.; Mumper, R. J. Paclitaxel nano-delivery systems: a comprehensive review. *Journal of nanomedicine & nanotechnology* **2013**, *4* (2), 1000164.
(72) Jagannathan, R.; Abraham, P. M.; Poddar, P. Temperature-dependent spectroscopic evidences of curcumin in aqueous medium: a mechanistic study of its solubility and stability. *J. Phys. Chem. B* **2012**, *116* (50), 14533−14540.
(73) Alavi, M.; Nokhodchi, A. Micro-and nanoformulations of paclitaxel based on micelles, liposomes, cubosomes, and lipid nanoparticles: Recent advances and challenges. *Drug Discovery Today* **2021**.
(74) Stohs, S. J.; Chen, O.; Ray, S. D.; Ji, J.; Bucci, L. R.; Preuss, H. G. Highly bioavailable forms of curcumin and promising avenues for curcumin-based research and application: A review. *Molecules* **2020**, *25* (6), 1397.
(75) He, Z. J.; Wan, X. M.; Schulz, A.; Bludau, H.; Dobrovolskaia, M. A.; Stern, S. T.; Montgomery, S. A.; Yuan, H.; Li, Z. B.; Alakhova, D.; Sokolsky, M.; Darr, D. B.; Perou, C. M.; Jordan, R.; Luxenhofer, R.; Kabanov, A. V. A high capacity polymeric micelle of paclitaxel: Implication of high dose drug therapy to safety and in vivo anti-cancer activity. *Biomaterials* **2016**, *101*, 296−309.
(76) Lübtow, M. M.; Oerter, S.; Quader, S.; Jeanclos, E.; Cubukova, A.; Krafft, M.; Haider, M. S.; Schulte, C.; Meier, L.; Rist, M.; Sampetrean, O.; Kinoh, H.; Gohla, A.; Kataoka, K.; Appelt-Menzel, A.; Luxenhofer, R. In Vitro Blood-Brain Barrier Permeability and Cytotoxicity of an Atorvastatin-Loaded Nanoformulation Against Glioblastoma in 2D and 3D Models. *Mol. Pharmaceutics* **2020**, *17* (6), 1835−1847.
(77) Luxenhofer, R.; Schulz, A.; Roques, C.; Li, S.; Bronich, T. K.; Batrakova, E. V.; Jordan, R.; Kabanov, A. V. Doubly amphiphilic poly(2-oxazoline)s as high-capacity delivery systems for hydrophobic drugs. *Biomaterials* **2010**, *31* (18), 4972−4979.
(78) Marzo, A.; Heftmann, E. Enantioselective analytical methods in pharmacokinetics with specific reference to genetic polymorphic metabolism. *J. Biochem. Bioph. Methods* **2002**, *54* (1−3), 57−70.
(79) Jamali, F. Pharmacokinetics of enantiomers of chiral non-steroidal anti-inflammatory drugs. *Eur. J. Drug Metab. Pharmacokinet.* **1988**, *13* (1), 1−9.
(80) Yalkowsky, S. H.; Dannenfelser, R. M. Aquasol database of aqueous solubility. College of Pharmacy, University of Arizona, Tucson, AZ. *College of Pharmacy, University of Arizona, Tucson, AZ.*1992; 189.*189*
(81) Yang, Y. Q.; Guo, X. D.; Lin, W. J.; Zhang, L. J.; Zhang, C. Y.; Qian, Y. Amphiphilic copolymer brush with random pH-sensitive/hydrophobic structure: synthesis and self-assembled micelles for sustained drug delivery. *Soft Matter* **2012**, *8* (2), 454−464.
(82) Heikkilä, T.; Salonen, J.; Tuura, J.; Hamdy, M.; Mul, G.; Kumar, N.; Salmi, T.; Murzin, D. Y.; Laitinen, L.; Kaukonen, A. M. Mesoporous silica material TUD-1 as a drug delivery system. *Int. J. Pharm.* **2007**, *331* (1), 133−138.
(83) Ali, A. E.; AlArifi, A. S. Swelling and Drug Release Profile of Poly(2-ethyl-2-oxazoline)-Based Hydrogels Prepared by Gamma Radiation-Induced Copolymerization. *J. Appl. Polym. Sci.* **2011**, *120* (5), 3071−3077.
(84) Kostova, B.; Ivanova-Mileva, K.; Rachev, D.; Christova, D. Study of the Potential of Amphiphilic Conetworks Based on Poly(2-ethyl-2-oxazoline) as New Platforms for Delivery of Drugs with Limited Solubility. *AAPS PharmSciTech* **2013**, *14* (1), 352−359.
(85) Medina, D. D.; Mastai, Y. Chiral Polymers and Polymeric Particles for Enantioselective Crystallization. *Isr. J. Chem.* **2018**, *58* (12), 1330−1337.
(86) Lim, C.; Ramsey, J. D.; Hwang, D.; Teixeira, S. C. M.; Poon, C.-D.; Strauss, J. D.; Rosen, E. P.; Sokolsky-Papkov, M.; Kabanov, A. V. Drug-Dependent Morphological Transitions in Spherical and Worm-Like Polymeric Micelles Define Stability and Pharmacological Performance of Micellar Drugs. *Small* **2022**, *18* (4), 2103552.

https://doi.org/10.1021/acs.macromol.2c00229
Macromolecules 2022, 55, 6176−6190